EARTH SURFACE PROCESSES AND LANDFORMS
Earth Surf. Process. Landforms **45**, 841–861 (2020)

Published online 3 February 2020 in Wiley Online Library
(wileyonlinelibrary.com) DOI: 10.1002/esp.4778

Interaction of wind and cold-season hydrologic processes on erosion from complex topography following wildfire in sagebrush steppe

Samantha P. Vega,[1,2] C. Jason Williams,[3]* Erin S. Brooks,[4] Frederick B. Pierson,[2] Eva K. Strand,[5] Peter R. Robichaud,[6] Robert E. Brown,[6] Mark S. Seyfried,[2] Kathleen A. Lohse,[7] Kayla Glossner,[7] Jennifer L. Pierce[8] and Clay Roehner[8]

[1] Department of Water Resources, University of Idaho, Moscow, Idaho USA
[2] Northwest Watershed Research Center, Agricultural Research Service, US Department of Agriculture, Boise, Idaho USA
[3] Southwest Watershed Research Center, Agricultural Research Service, US Department of Agriculture, Tucson, Arizona USA
[4] Department of Soil and Water Systems, University of Idaho, Moscow, Idaho USA
[5] Department of Forest, Rangeland, and Fire Sciences, University of Idaho, Moscow, Idaho USA
[6] Moscow Forest Sciences Laboratory, Rocky Mountain Research Station, Forest Service, US Department of Agriculture, Moscow, Idaho USA
[7] Department of Biological Sciences, Idaho State University, Pocatello, Idaho USA
[8] Department of Geosciences, Boise State University, Boise, Idaho USA

Received 28 February 2019; Revised 18 November 2019; Accepted 25 November 2019

*Correspondence to: C. Jason Williams, Southwest Watershed Research Center, Agricultural Research Service, US Department of Agriculture, 2000 East Allen Road, Tucson, AZ 85719, USA. E-mail: jason.williams@usda.gov

ESPL
Earth Surface Processes and Landforms

ABSTRACT: Wildfire is a natural component of sagebrush (*Artemisia* spp.) steppe rangelands that induces temporal shifts in plant community physiognomy, ground surface conditions, and erosion rates. Fire alteration of the vegetation structure and ground cover in these ecosystems commonly amplifies soil losses by wind- and water-driven erosion. Much of the fire-related erosion research for sagebrush steppe has focused on either erosion by wind over gentle terrain or water-driven erosion under high-intensity rainfall on complex topography. However, many sagebrush rangelands are geographically positioned in snow-dominated uplands with complex terrain in which runoff and sediment delivery occur primarily in winter months associated with cold-season hydrology. Current understanding is limited regarding fire effects on the interaction of wind- and cold-season hydrologic-driven erosion processes for these ecosystems. In this study, we evaluated fire impacts on vegetation, ground cover, soils, and erosion across spatial scales at a snow-dominated mountainous sagebrush site over a 2-year period post-fire. Vegetation, ground cover, and soil conditions were assessed at various plot scales (8 m^2 to 3.42 ha) through standard field measures. Erosion was quantified through a network of silt fences (n = 24) spanning hillslope and side channel or swale areas, ranging from 0.003 to 3.42 ha in size. Sediment delivery at the watershed scale (129 ha) was assessed by suspended sediment samples of streamflow through a drop-box v-notch weir. Wildfire consumed nearly all above-ground live vegetation at the site and resulted in more than 60% bare ground (bare soil, ash, and rock) in the immediate post-fire period. Widespread wind-driven sediment loading of swales was observed over the first month post-fire and extensive snow drifts were formed in these swales each winter season during the study. In the first year, sediment yields from north- and south-facing aspects averaged 0.99–8.62 t ha^{-1} at the short-hillslope scale (~0.004 ha), 0.02–1.65 t ha^{-1} at the long-hillslope scale (0.02–0.46 ha), and 0.24–0.71 t ha^{-1} at the swale scale (0.65–3.42 ha), and watershed scale sediment yield was 2.47 t ha^{-1}. By the second year post fire, foliar cover exceeded 120% across the site, but bare ground remained more than 60%. Sediment yield in the second year was greatly reduced across short- to long-hillslope scales (0.02–0.04 t ha^{-1}), but was similar to first-year measures for swale plots (0.24–0.61 t ha^{-1}) and at the watershed scale (3.05 t ha^{-1}). Nearly all the sediment collected across all spatial scales was delivered during runoff events associated with cold-season hydrologic processes, including rain-on-snow, rain-on-frozen soils, and snowmelt runoff. Approximately 85–99% of annual sediment collected across all silt fence plots each year was from swales. The high levels of sediment delivered across hillslope to watershed scales in this study are attributed to observed preferential loading of fine sediments into swale channels by aeolian processes in the immediate post-fire period and subsequent flushing of these sediments by runoff from cold-season hydrologic processes. Our results suggest that the interaction of aeolian and cold-season hydrologic-driven erosion processes is an important component for consideration in post-fire erosion assessment and prediction and can have profound implications for soil loss from these ecosystems. © 2019 John Wiley & Sons, Ltd.

KEYWORDS: cold-season hydrology; fire effects; hillslope processes; rangeland hydrology; sagebrush; sediment production; sediment yield; silt fence; snowmelt runoff; wind erosion

Introduction

Sagebrush (*Artemisia* spp.) rangelands span a vast expanse (>300 000 km^2) of the semi-arid western USA inclusive of rain-dominated valley areas and snow-dominated uplands with complex terrain (Miller et al., 2011; Seyfried et al., 2018). Annual sediment yields from these rangelands are commonly low due to a 'resource-conserving' vegetation and ground cover structure that limits connectivity of runoff and erosion processes (Seyfried and Wilcox, 1995; Wilcox et al., 2003; Pierson et al., 2008a, 2009; Williams et al., 2016a). The physiognomy of undisturbed sagebrush hillslopes is patchy, with bare areas intermingled in a mosaic of bunchgrasses and sagebrush shrub islands underlain by a variable-thickness litter layer (Hironaka et al., 1983; Johnson and Gordon, 1988; Blackburn et al., 1992; Pierson et al., 1994a; Davies and Bates, 2010). This vegetation and ground cover structure buffers rainfall intensity, facilitates infiltration, and inhibits the downslope transport of sediment detached by raindrops and isolated overland flow (Johnson and Blackburn, 1989; Pierson et al., 1994b, 2008a, 2008b, 2009; Seyfried and Wilcox, 1995). Field studies of high-intensity rainfall simulations (32.5 m^2 plots) on these lands report low event sediment yields, ranging from near 0 to <0.1 t ha^{-1} (Johnson and Blackburn, 1989; Pierson et al., 2009; Pierson and Williams, 2016). Runoff from snow-dominated sagebrush uplands occurs primarily during the spring snowmelt season as streamflow, but hillslope runoff does occur during winter rainfall events on frozen soil or snow (Blackburn et al., 1990; Pierson and Wight, 1991; Seyfried and Wilcox, 1995; Pierson et al., 2001a; Godsey et al., 2018). The quantity and timing of runoff from these systems are strongly regulated by the amount and distribution of accumulated snow, the onset and duration of the snowmelt period, soil water conditions, and above- and below-ground hillslope hydrologic connectivity (McNamara et al., 2005; Seyfried et al., 2009; Williams et al., 2009; Nayak et al., 2010; Chauvin et al., 2011; McNamara et al., 2018). Snowfall in sloping sagebrush uplands is commonly redistributed into extensive drifts that dictate the water available for runoff and that regulate the length of the runoff period (Flerchinger and Cooley, 2000; Winstral et al., 2013; Kormos et al., 2017). Hillslope soil loss from snowmelt runoff is generally minimal for well-vegetated sagebrush uplands, and the bulk of annual watershed sediment yields (~1–2 t ha^{-1} yr^{-1}) for these sites comes from in-channel processes during the highest flows (Pierson et al., 2001a; Pierson and Williams, 2016). There are few wind erosion studies of well-vegetated sagebrush rangelands, but recent work suggests erosion by wind processes is minimal for these landscapes in the absence of disturbance (Sankey et al., 2009a, 2009b, 2012a, 2012b; Wagenbrenner et al., 2013).

Fire effects on vegetation and ground cover structure in sagebrush steppe decrease the amount of rainfall input necessary to generate runoff and detach sediment, and increase sediment availability and connectivity of runoff and erosion processes (Pierson et al., 2001b, 2002, 2008a, 2009, 2011; Al-Hamdan et al., 2012; Williams et al., 2014a, 2016a). The impact of fire on hillslope runoff generation and sediment yield during rainfall on sloping sagebrush rangelands is commonly exacerbated by hydrophobic soil conditions inherent to these systems (Salih et al., 1973; Pierson et al., 2008b, 2009; Glenn and Finley, 2010; Williams et al., 2016b). At a sagebrush site in Nevada, USA, Pierson et al. (2001b, 2008a, 2008b) found that temporal variability in background soil water repellency exerted a greater influence on fine-scale (0.5 m^2 plots) runoff responses during rainfall simulations than burning did the first 2 years post fire, but minimum infiltration rates were lower and cumulative sediment yields were 3- to 14-fold greater for burned than unburned sagebrush shrub microsites with strongly water-repellent soils. In another rainfall simulation study, Pierson et al. (2009) reported similar results for soil water repellency, runoff, and sediment yield on sagebrush shrub microsites (0.5 m^2 plots) 1 year post fire. Pierson et al. (2009) further found that fire removal of vegetation and ground cover along with persistence of strong soil water repellency reduced time to runoff and increased runoff by sixfold and sediment yield by more than 125-fold on 32.5 m^2 (patch-scale) rainfall simulation experiments conducted in the immediate post-fire period. The authors determined that runoff and sediment generated by rainsplash and sheetflow at the fine spatial scale on burned plots (183–705 g m^{-2}, 1.8–7.1 t ha^{-1}) formed into high-velocity concentrated overland flow or rills over the patch scale and that the higher velocity flows on burned (0.11–0.20 m s^{-1}) than unburned (0.07–0.16 m s^{-1}) plots detached and transported substantially more sediment (988 g m^{-2}, 9.9 t ha^{-1}) than measured on unburned plots without rills (8 g m^{-2}, 0.1 t ha^{-1}) (Pierson et al., 2009). Runoff from burned plots (16 mm) at the patch scale returned to near that of unburned plots (3 mm) 1 year post fire due in part to reduced soil water repellency strength, whereas sediment yield declined to the unburned level 2 years post fire due to reduced bare ground and limited runoff (Pierson et al., 2009). Similar hydrologic and erosion responses and controls on post-fire erosion risk have been reported in other plot-scale studies of burned sagebrush rangelands in complex terrain (Pierson et al., 2002; Williams et al., 2016b). Studies of streamflow from burned sagebrush rangelands are limited in the literature, but numerous anecdotal reports document amplified streamflow, extensive flooding, soil loss, debris flows, and damage to values-at-risk following burning of sloping sagebrush steppe (Pierson et al., 2002, 2011; Williams et al., 2014a). Collectively, the studies noted above demonstrate that burning of sloping sagebrush rangelands reduces the inherent 'resource-conserving' vegetation structure on these landscapes and thereby amplifies the potential for runoff and erosion associated with increased connectivity of runoff and erosion sources and processes across spatial scales (e.g., Williams et al., 2016a). These first-order fire effects on runoff and water-driven erosion on sagebrush rangelands are consistent with those commonly reported for burned rangelands, woodlands, and dry forests around the world (Cannon et al., 2001; Cerdà and Doerr, 2005; Shakesby and Doerr, 2006; Moody et al., 2013; Shakesby, 2011; Williams et al., 2014b). Estimates from burned semi-arid forests suggest first year post-fire sediment yield across the hillslope to watershed scales can approach 60–100 t ha^{-1} (Spigel and Robichaud, 2007; Robichaud, 2009).

Recent advancements in understanding of fire impacts on aeolian processes demonstrate that wind erosion is a substantial sediment transport mechanism on rangelands post fire and that wind erosion may be a particularly important process in sagebrush steppe (Sankey et al., 2009a, 2009b, 2012a, 2012b; Hasselquist et al., 2011; Wagenbrenner et al., 2013). Sankey et al. (2009a) conducted a meta-analysis of fire effects studies on wind erosion from rangeland systems and determined sediment capture from burned rangelands was nearly 30- to more than 160-fold more than from unburned rangelands in the pooled analysis. In that study, the authors also evaluated fire impacts on wind transport of sediment from burned and unburned areas at sagebrush steppe sites for a period of 323 days, initiated about 45 days following wildfire. Sankey et al. (2009a) reported sediment transport averages of 0.0250 and 0.0051 g d^{-1} for burned conditions and 0.0004 and 0.0002 g d^{-1} for unburned conditions as measured with passive sediment collectors, respectively, at low (0.2 m) and high (0.55 m) collection heights above the ground surface.

The 30-day measured horizontal mass transport was negligible for unburned areas and averaged 5.40, 2.80, and 0.32 kg m^{-1} for burned areas the first, second, and third months of sampling, representative of the dry autumn and early cool winter periods (Sankey et al., 2009a). Wind erosion decreased thereafter due to herbaceous vegetation recovery in spring months, with the exception of minor episodic sediment transport during the following summer dry period (Sankey et al., 2009a). Wagenbrenner et al. (2013) reported that extensive bare and dry conditions facilitated high levels of wind erosion from a burned sagebrush site in Idaho, USA, the first 2 months post fire, with the largest event generating 1495 kg m^{-1} horizontal sediment transport as measured over 13 days. The 11-month study found wind erosion subsequently dampened from initial high levels due to a brief autumn rainy period, increased slightly (120.4 kg m^{-1}, over 2 weeks) before winter snowfall, was limited to several events after snowmelt (136.8 kg m^{-1}, 9 days), and then declined to negligible levels with vegetation regrowth the first spring after fire (Wagenbrenner et al., 2013). Studies by Sankey et al. (2009a, 2009b, 2012a) and Wagenbrenner et al. (2013) collectively demonstrate that wind erosion following burning on sagebrush rangelands is substantial and highest immediately post fire, declines with increased soil moisture during autumn rains and winter snowfall, and is negligible over time due to vegetation recovery.

Recent increases in wildfire activity across much of the sagebrush steppe domain in the western USA necessitates improved understanding of the interaction in wind- and water-driven erosion processes (Pierson et al., 2011; Williams et al., 2014a; Edwards et al., 2019). Invasions of low- to mid-elevation sagebrush rangelands by the fire-prone annual cheatgrass (*Bromus tectorum* L.) have substantially shorted fire return intervals (by 10-fold in some areas), and fires at these elevations commonly move upslope into adjacent snow-dominated sagebrush uplands, where fire activity is also projected to increase (Miller et al., 2011; Balch et al., 2013; Williams et al., 2014a; Snyder et al., 2019). This increasing role of wildfire in sagebrush steppe has major ecohydrologic and economic ramifications for values-at-risk and potentially increases long-term soil loss from these rangelands (Pierson et al., 2011; Wilcox et al., 2012; Williams et al., 2014a; Edwards et al., 2019) Although knowledge of fire effects on hillslope hydrology and water-driven erosion is well documented (e.g., Pierson and Williams, 2016), understanding regarding fire impacts on watershed-scale streamflows and sediment yield from sagebrush rangelands remains limited. Knowledge of fire effects on erosion by wind in sagebrush steppe has greatly advanced in the past decade, but much of the understanding is from research on gently sloping terrain (Sankey et al., 2009a, 2009b, 2012a, 2012b; Wagenbrenner et al., 2013). A key knowledge gap remains regarding the interaction of wind- and water-driven erosion processes following wildfire on sagebrush rangelands in complex topography. In particular, very little is known about how pulses of sediment detached by wind and subsequently deposited in the immediate post-fire period contribute to water-driven sediment delivery across spatial scales in these systems. This study aims to improve understanding of fire impacts on erosion from sagebrush rangelands associated with interaction of wind and cold-season hydrologic processes across the hillslope to watershed scales in complex topography. To address this goal, we evaluated fire impacts on vegetation, ground cover, soils, and erosion across hillslope to watershed spatial scales over a 2-year period after wildfire through a suite of field measurements and *in situ* hydrometric measures. The study was conducted on a burned sagebrush site with a snow-dominated precipitation regime and complex terrain and that underwent substantial redistribution of sediment by aeolian process in the first month after wildfire. Specific objectives included: (a) to quantify initial vegetation, ground cover, and soil water repellency conditions immediately post fire; and (b) to quantify changes in vegetation, ground cover, soil water repellency, and sediment delivery over each of 2 years following wildfire. Vegetation, ground cover, and soil water repellency were assessed at various plot scales through standard field measures. Erosion was quantified through a network of silt fences spanning hillslope and side channel or swale areas, ranging from 0.003 to 3.415 ha in size. Sediment delivery at the watershed scale (129 ha) was assessed by suspended sediment samples of streamflow through a pre-existing drop-box v-notch weir. Although our study focuses specifically on the sagebrush steppe ecosystem, the study provides insight for similar fire-prone semi-arid rangelands, woodlands, and dry forests around the world.

Methods

Study area

This study was conducted within the Murphy Creek Watershed in the Owyhee Mountains of southwestern Idaho, located approximately 90 km from the city of Boise. The Murphy Creek Watershed is part of a network of research sub-watersheds in the larger Reynolds Creek Experimental Watershed (23 900 ha, RCEW) administered by the US Department of Agriculture, Agricultural Research Service, Northwest Watershed Research Center (USDA-ARS-NWRC; Slaughter et al., 2001). RCEW comprises the Reynolds Creek Critical Zone Observatory (RCEW-CZO) (Seyfried et al., 2018) and is extensively instrumented to support research on a wide range of hydrologic phenomena, soil erosion processes, soil carbon storage and flux, fire impacts, and changes in vegetation (Hanson, 2001; Pierson et al., 2001a, 2009; Nayak et al., 2010; Chauvin et al., 2011; Marks et al., 2013; Williams et al., 2016b; Godsey et al., 2018; Kormos et al., 2018). Our specific study area, the Murphy Creek Experimental Watershed (MCEW), is defined as the watershed area contributing to the south fork of Murphy Creek immediately upstream of the USDA-ARS-NWRC Murphy Creek Weir (43° 15′ 20.2″ N latitude, 116° 49′ 10.3″ W longitude, 1390 m MSL; Figure 1). The study area and approximately 25% of the surrounding RCEW were burned by the Soda Fire in 2015. The wildfire was initiated by a lightning strike on 15 August 2015 during dry summer conditions and subsequently burned more than 110 000 ha, much of which was sagebrush steppe (USDI-BLM, 2016). The fire consumed nearly all of the above-ground vegetation in the MCEW, leaving behind a mosaic of burned shrub skeletons and plant bases, charred litter, ash, bare soil, and rock (Figure 2). Burn severity was classified as moderate for most of the study area (Figure 3). Field reconnaissance observed considerable redistribution of wind-detached sediment and organic debris into hillslope hollows or swales throughout MCEW over the first month after the fire (Figure 4; Vega, 2018). Sediment and debris redistribution by aeolian processes during this period were not quantified for logistical reasons, but field-observed trends in wind erosion and subsequent sediment and debris deposition were consistent with those reported for the immediate post-fire period in numerous wind erosion studies of sagebrush steppe (Sankey et al., 2009a, 2009b, 2012a, 2012b; Wagenbrenner et al., 2013).

Pre-fire watershed biophysical attributes for the MCEW are available from previous studies by the USDA-ARS-NWRC (Hanson, 2000, 2001; Pierson et al., 2000, 2001a; Seyfried et al., 2001; Vega, 2018) and others (Stephenson, 1977). The MCEW is elongated in shape, oriented predominantly with

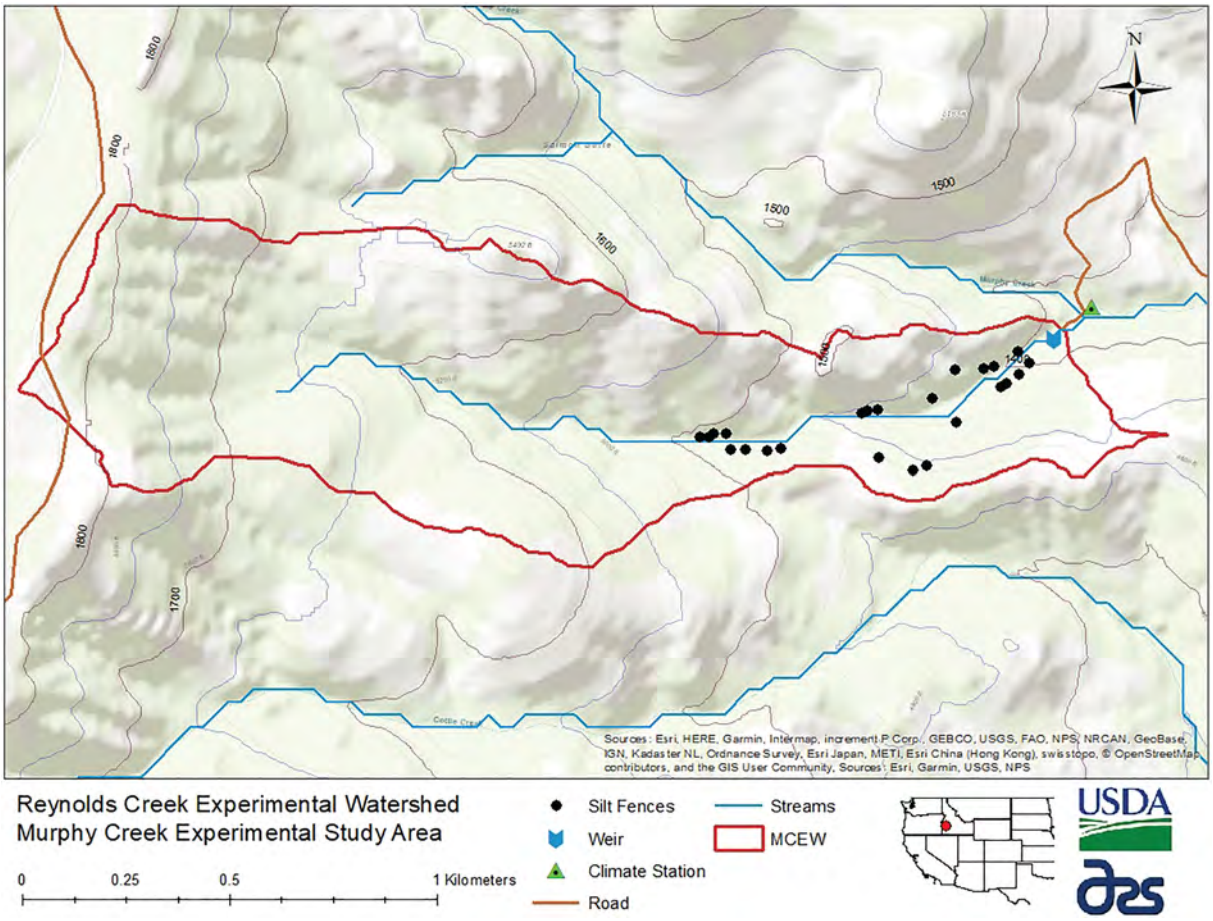

Figure 1. Map of the Murphy Creek Experimental Watershed (43° 15′ 20.2″ N latitude, 116° 49′ 10.3″ W longitude, 1390 m MSL) study area and instrumentation (silt fences, weir, and climate station) located along the South Fork of Murphy Creek and upslope of the Murphy Creek Weir in the Reynolds Creek Experimental Watershed, administered by the US Department of Agriculture (USDA), Agricultural Research Service (ARS), Northwest Watershed Research Center, in southwestern Idaho, USA.

north- and south-facing hillslope aspects, and with numerous side channels and hillslope hollows/swales (Figures 1 and 2). Elevation across the watershed ranges approximately from 1388 to 1823 m above MSL. Hillslopes generally range from 60 to 400 m in length, with a 25–45% slope gradient (Vega, 2018). Hillslopes are underlain by basalt and tuff bedrock (Seyfried et al., 2001). Soils on north-facing hillslopes are loams to clay loams with an average depth of 88 cm (Stephenson, 1977). Soils on south-facing hillslopes are well-drained stony, gravelly, and very stony clay loams and are generally rockier and shallower (48 cm to bedrock) than on north-facing hillslopes (Stephenson, 1977). Precipitation in most years ranges from approximately 450 mm at lower elevations to 800 mm at upper elevations, and occurs predominantly as snowfall (~60% of annual) in most years (Hanson, 2000, 2001). Average annual air temperature approximates 7.9°C based on RCEW meteorological stations at similar elevations to MCEW (Hanson, 2001). Streamflow through the watershed is spring fed and intermittent, with peak flows during winter rain-on-snow events and the spring snowmelt period (Pierson et al., 2001a). The USDA-ARS-NWRC long-term stream discharge database reports mean annual streamflow from the watershed at 191.7 mm (7.52 L s^{-1}, 0.008 m^3 s^{-1}), as measured at the drop-box v-notch weir on the south fork of Murphy Creek (hereafter Murphy Creek Weir, 1967–1977 period of record; Pierson et al., 2000, 2001a). Hillslope vegetation prior to the fire was typical for uplands dominated by mountain big sagebrush (*A. tridentata* Nutt. ssp. *vaseyana* [Rydb.] Beetle.) and bunchgrasses. Shrub cover consisted mainly of mountain big sagebrush, antelope bitterbrush (*Purshia tridentata* [Pursh] DC.), common snowberry (*Symphoricarpos albus* [L.] S.F. Blake), rabbitbrush (*Chrysothamnus viscidiflorus* [Hook.] Nutt.) and low sagebrush (*A. arbuscula* Nutt.). Herbaceous cover consisted primarily of Idaho fescue (*Festuca idahoensis* Elmer), bluebunch wheatgrass (*Pseudoroegneria spicata* [Pursh] Á. Löve), Sandberg bluegrass (*Poa secunda* J. Presl), and foxtail barley (*Hordeum jubatum* L.) grasses and various forbs (Pierson et al., 2000; Seyfried et al., 2001).

Experimental design

A suite of experimental plots were combined with a USDA-ARS-NWRC instrument network in the MCEW to quantify vegetation and soil conditions, hillslope erosion, precipitation input, and watershed-scale streamflow and sediment delivery over a 2-year period (autumn 2015 to summer 2017) after the Soda Fire. Experimental plots were established on north- and south-facing hillslopes to quantify vegetation, ground cover, soil water repellency, and sediment yield at multiple spatial scales. Owing to land ownership within the watershed, experimental plots were restricted to the lower third of the drainage, upstream of the Murphy Creek Weir (Figure 1). Field reconnaissance immediately post fire found hillslope vegetation and ground-surface conditions in the experimental area were generally consistent with those of the remainder of the watershed (Vega, 2018). Maps of pre-fire vegetation and soils in the watershed (Seyfried et al., 2000, 2001) indicate that the experimental hillslopes are representative of hillslopes in the remainder of the watershed upstream from the weir. An array (or block) of silt

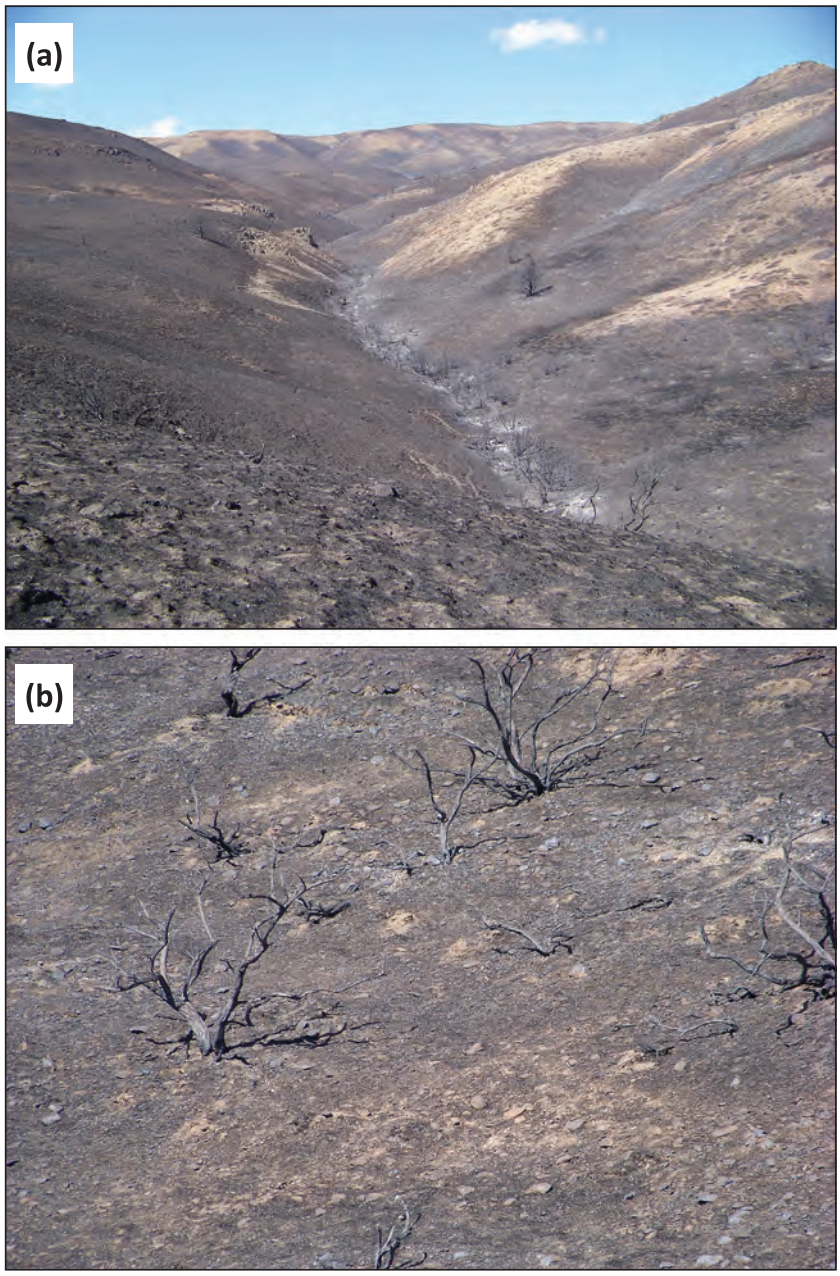

Figure 2. Photographs of the Murphy Creek Experimental Watershed study area upstream of the Murphy Creek Weir and along the South Fork of Murphy Creek approximately 21 days after burning in the Soda Fire on 15 August 2015. Foreground and left side of panel (a) show burned vegetation and ground surface conditions on north-facing hillslopes, and panel (b) shows burned shrub skeletons and the rocky burned surface typical of south-facing hillslopes in the watershed at the initiation of this study. Photo credits: C. Jason Williams, US Department of Agriculture, Agricultural Research Service. [Colour figure can be viewed at wileyonlinelibrary.com]

fence plots (see Robichaud and Brown, 2002) was installed on three different hillslopes on north- and on south-facing aspects within the experimental area to quantify sediment yield (Figures 1, 5, and 6). Each array consisted of two short-hillslope plots bounded 10–13 m upslope by a hand-dug trench, one long-hillslope plot bounded ~100 m (106 m on average) upslope by a topographic break, and one swale plot bounded ~250 m upslope (246 m on average) by the hillslope/drainage divide (Figure 5). The different plot types and sizes were installed to quantify sediment delivery at different spatial scales associated with scale-dependent erosion processes (e.g., interrill, rill, hillslopes versus swales). Sediment from natural runoff events for each plot type was collected in a silt fence at the base of the plot and subsequently sampled. Silt fence installations were initiated on 16 September 2015 on north-facing hillslopes and were fully complete across all hillslopes on 12 November 2015. There were no runoff-generating rainfall events in the watershed during the silt fence installation period. Vegetation, ground cover, soil water repellency, and surface microtopography were quantified for short-hillslope plots immediately after plot installation in autumn 2015 and in summers of 2016 and 2017 using methods described below. Vegetation and ground cover on long-hillslope and swale plots were quantified in summer 2016 and summer 2017 as described below.

Precipitation input into the watershed and site meteorological conditions during the study were determined based on three USDA-ARS-NWRC climate–meteorological stations: (a) the Murphy Creek Watershed Station (Site ID 043b; see Figure 1), located ~100 m downslope from the Murphy Creek Weir; (b) the nearby (~9 km to the south, 1533 m MSL) Whiskey Mountain Station located within RCEW (Site ID 095b); and (c) the Johnston Draw Station (Site ID 125, ~15 km to the south, 1508 m MSL) (USDA-ARS-NWRC, 2015, 2016, 2017). The

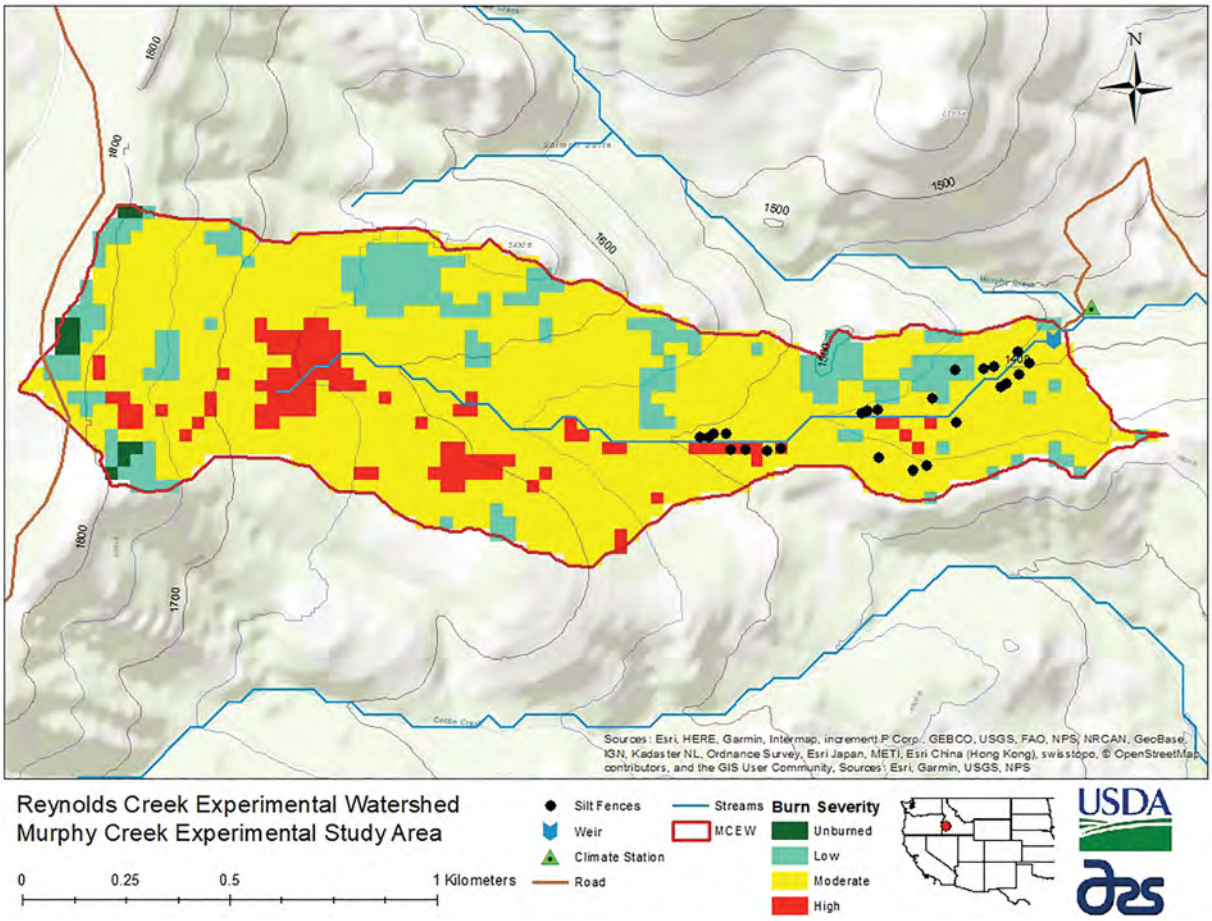

Figure 3. Map of burn severity and experimental instrumentation in the Murphy Creek Experimental Watershed immediately after the 2015 Soda Fire, as derived from burned area reflectance classification data (BARC) by the US Department of Interior, available online from the US Department of Agriculture (USDA) Geospatial Technology and Applications Center at: https://www.fs.fed.us/eng/rsac/baer/baer_request.html

Murphy Creek Watershed Station was established in the months following the Soda Fire and therefore the record for that station is incomplete over our full study period. Vega (2018) used standard regression techniques (Ott and Longnecker, 2010) to compile precipitation input and air temperature values for the MCEW for 1 October 2015 to 1 October 2017 using data from Whiskey Mountain Station. Our study utilizes the Vega (2018) dataset to characterize precipitation input and air temperatures in the MCEW throughout the study period. Data from the Johnston Draw Station are used to assess timing of frozen soils in the MCEW, as described by Vega (2018). Streamflow and sediment discharge at the watershed scale for the study period were quantified using data from the existing Murphy Creek Weir (Pierson et al., 2000, 2001a; USDA-ARS-NWRC, 2015, 2016, 2017; Vega, 2018). The Murphy Creek Weir was not operational at the time of the Soda Fire, but operations were re-established in autumn 2015 at the onset of streamflow. Stream stage is measured (10 s intervals) in a stilling well at the weir using a float with a Handar Shaft encoder and is logged using a CR1000 electronic datalogger (Campbell Scientific, Inc., Logan, UT, USA). Stage height in the stilling well is used to create a digital record of streamflow using weir calibration equations. Suspended sediment at the weir is sampled using a datalogger (CR1000)-controlled Sigma 900 automated pump sampler (Hach Company, Loveland, CO, USA). Collected sediment samples are subsequently filtered and weighed in the laboratory to determine sediment concentration of each sample. Both stage height and suspended sediment are intensely sampled during all events and periodically sampled during low flows. Detailed descriptions of streamflow and suspended sediment data collection and management for the Murphy Creek Weir are provided in Pierson et al. (2000, 2001a) for years 1967–1977 and in Vega (2018) for the period since the 2015 Soda Fire. Instantaneous sediment concentration data collected from the Murphy Creek Weir in this study were converted to daily sediment loading using the LOAD ESTimator (LOADEST) tool (Runkel et al., 2004), as described in Vega (2018). LOADEST uses regression techniques to establish relationships between streamflow, sediment data, and time or season within a year. The LOADEST tool then applies these relationships to estimate daily sediment load leaving the Murphy Creek Weir. Continuous sediment loads were estimated using the adjusted maximum likelihood estimation method within LOADEST.

Silt fence designs, installation, and sampling

All silt fences were designed and installed in a 'U' shape (Figure 6), transverse to the slope, using methods adapted from Robichaud and Brown (2002). Silt fences on short-hillslope plots were 3 m wide × 2 m long (Figure 6a). The contributing area of short-hillslope plots (31–46 m^2; 0.003–0.005 ha) was dictated by the aforementioned border trench 10–13 m upslope of the fence. Upslope border trenches were constructed to limit transfers of upslope material across the width of the silt fences. The trenches were oriented perpendicular to the hillslope profile, but with a slight downslope trend for drainage (Robichaud and Brown, 2002). Long-hillslope plots were installed with a 5 m wide × 2 m long silt fence as the downslope base and contributing areas ranging from 0.016 to 0.460 ha (Figures 5, 6c, and 6d). Swale plots were installed with two silt fences as the

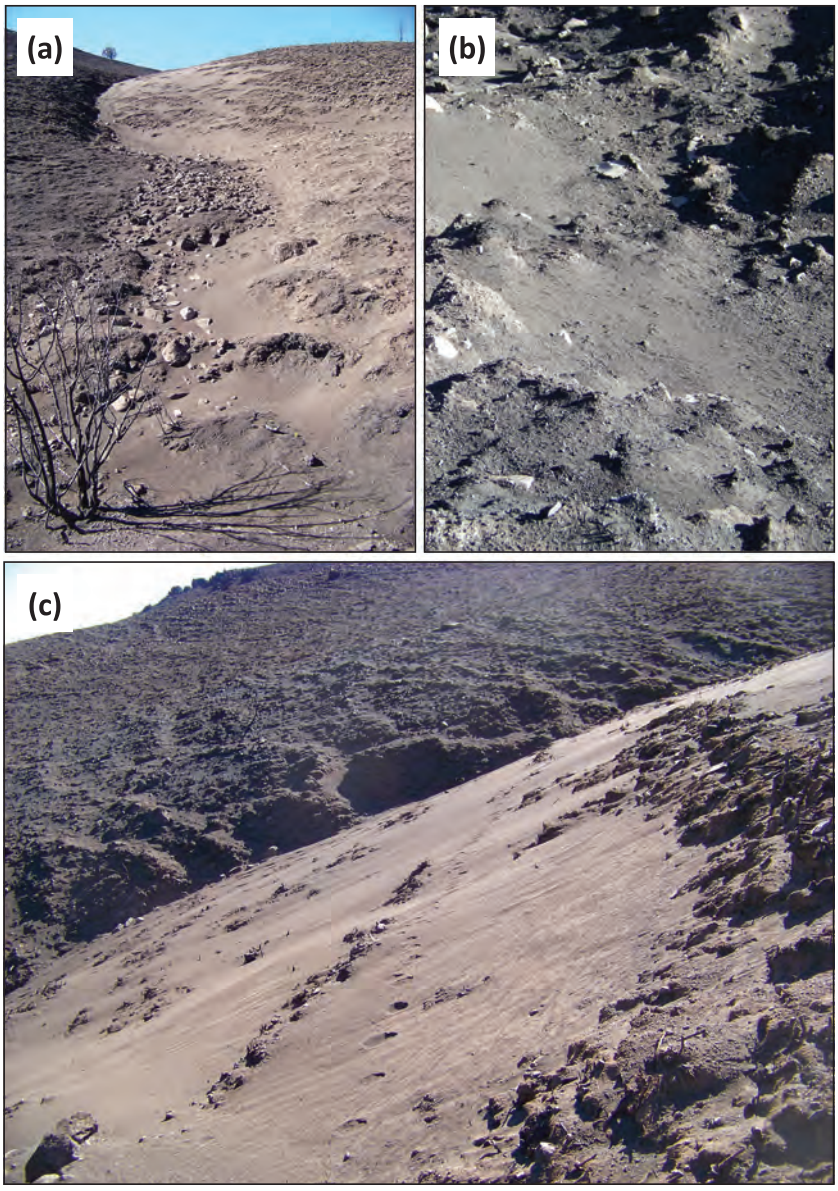

Figure 4. Photographs, taken on 21 September 2015, of sediment deposited by aeolian processes as commonly observed in the Murphy Creek Experimental Watershed in the first month following the 2015 Soda Fire. Panel (a) shows aeolian sediment deposition within a swale on a north-facing hillslope, panel (b) shows the sediment deposits in roughness elements within the swale, and panel (c) shows sediment deposition along side slopes of a swale on a north-facing hillslope. Photo credits: C. Jason Williams, US Department of Agriculture, Agricultural Research Service. [Colour figure can be viewed at wileyonlinelibrary.com]

downslope base (Figures 5 and 6b). We anticipated that more runoff would be directed through the swale plots, and therefore we installed a dual fence system to capture any overflow from the uppermost fence. Silt fences for swale plots were 1–5 m wide × 1–2 m long, with size dictated by swale width, and had contributing areas ranging from 0.654 to 3.415 ha. For each fence installation, the ground surface to be covered by silt fence fabric was cleared of any burnt shrubs and debris. Wooden or steel fence posts were pounded into place to frame side walls and the downslope end of each silt fence. Additional fence posts were driven into the ground approximately 1–2 m apart along the side wall and downslope ends of the silt fence to frame and further support the silt fence fabric. Contributing areas to short-hillslope plots were measured in the field using standard measuring tapes. Contributing areas to long-hillslope and swale silt fence plots were measured using the D8 flow routing routines in ArcGIS Desktop (Version 10.4.1; ESRI, 2016) with a 1 m spatial resolution LIDAR-derived digital elevation model of the study area (Ilangakoon et al., 2016) and geo-referenced silt fence locations (Vega, 2018).

This study used Lumite silt fence fabric (Shaw Fabric Products, Loveland, CO, USA). The fabric was selected for its durability, sediment trapping capabilities, and permeability (Robichaud and Brown, 2002; Benavides-Solorio and MacDonald, 2005). Lumite fabric has a tensile strength of 0.78 kN × 0.51 kN, a puncture strength of 0.31 kN, and a permeability of 611 L m^{-2} min^{-1}. The fabric was spread out along each fence post structure and attached to the fence posts using roofing nails or bailing wire. Excess fabric at the base of fence posts was routed along the ground surface (in the upslope direction) and anchored into the ground using 8-gauge (203 mm long × 51 mm wide) fabric staples. Additional pieces of fabric were overlain to cover the soil surface and excess fabric was anchored into the ground with the fabric staples. Lastly, a trench was excavated ~10–15 cm deep along the upslope end of the fence location, and a final piece

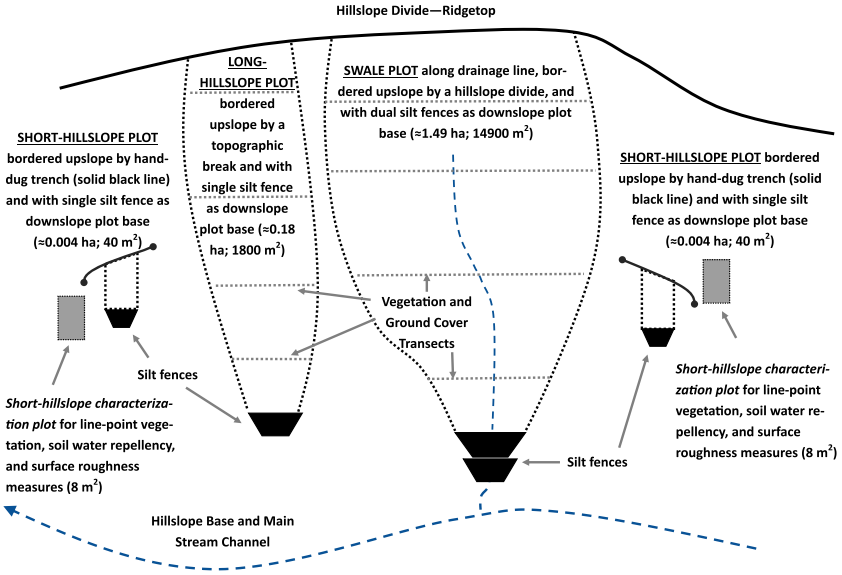

Figure 5. Diagram of a typical silt fence array or block employed in this study on north-facing (n = 3 blocks) and south-facing (n = 3 blocks) hillslopes of the Murphy Creek Experimental Watershed. Each individual block contained two short-hillslope plots bounded (dashed black lines) 10–13 m upslope by a hand-dug trench (solid dark grey black bars), one long-hillslope plot bounded (dashed black lines) ~100 m upslope by a topographic break, and one swale plot bounded (dashed black lines) ~250 m upslope by the hillslope divide (solid black line). The different plot types and sizes were installed to quantify sediment delivery at different spatial scales associated with scale-dependent erosion processes. Sediment from natural runoff events for each plot type was collected in one (short- and long-hillslope plots) or two (swale plots) silt fences (black polygons) at the plot base. Vegetation, ground cover, soil water repellency, and surface roughness for each short-hillslope plot were assessed on a 2 m × 4 m short-hillslope characterization plot (grey rectangles) immediately adjacent to the respective silt fence location so as not to disturb the silt fence plot area. Vegetation and ground cover on each long-hillslope and each swale plot were measured along four transects (dashed grey lines) oriented parallel to the hillslope contour and evenly spaced within the respective plot area as shown. Diagram not drawn to scale. [Colour figure can be viewed at wileyonlinelibrary.com]

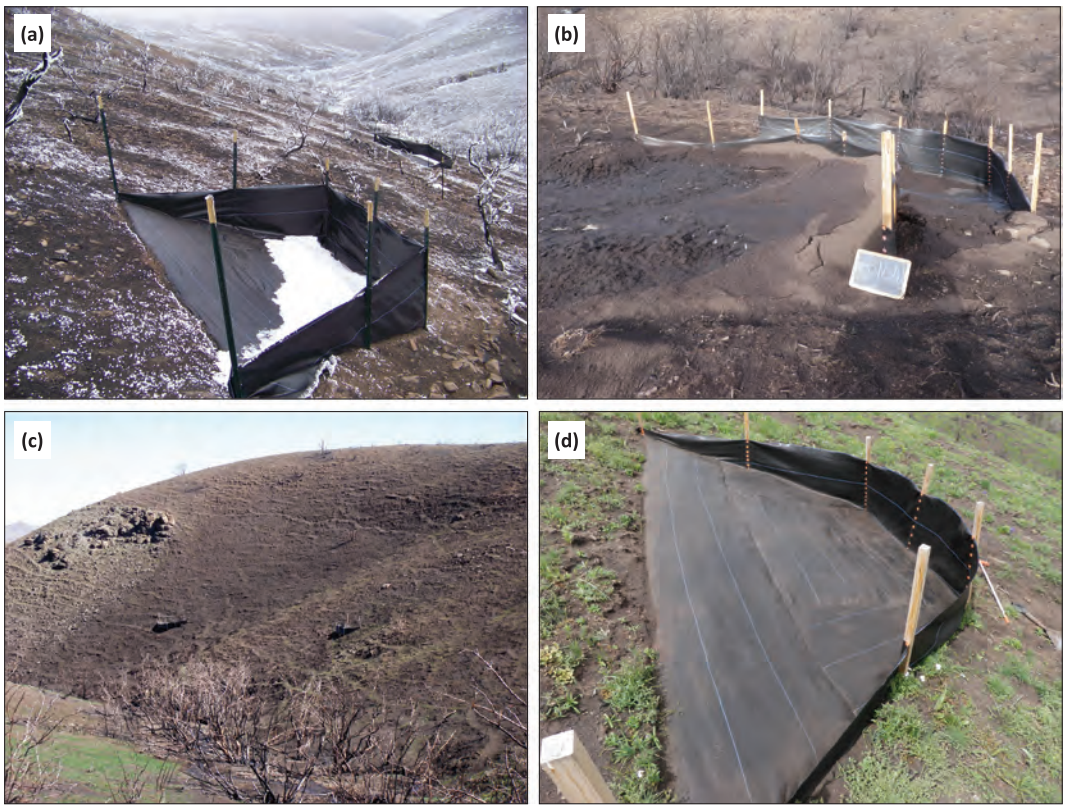

Figure 6. Photographs of silt fence designs in the Murphy Creek Experimental Watershed installed in the months following the 15 August 2015 Soda Fire. Panel (a) shows a short-hillslope plot silt fence on a south aspect with frozen soils in late November 2015; panel (b) shows the dual silt fence design in a swale plot on a north-facing hillslope, with sediment from runoff of rainfall on frozen soils as observed in late November 2015; panel (c) shows a north-facing hillslope with one long-hillslope plot and one short-hillslope plot in early April 2015 (~9 months post fire); and panel (d) shows a long-hillslope plot silt fence on a north-facing aspect in May 2016, approximately 10 months post fire. Photos by US Department of Agriculture, Agricultural Research Service, Northwest Watershed Research Center. [Colour figure can be viewed at wileyonlinelibrary.com]

of fabric was laid over the trench on the uphill side of the fence and backfilled and stapled into the trench to anchor the fabric in place (Robichaud and Brown, 2002). This final piece of fabric was then laid back over the trench on to the remaining plot surface downslope and further anchored into the ground with fabric staples.

Silt fences were field monitored bi-weekly to monthly, depending on precipitation events, to assess sediment accumulation. The fences were cleaned out as needed to quantify sediment delivered from hillslopes and swales. Accumulated sediment within fences was measured during each cleanout by bucket weighing all removed sediment on site (Robichaud and Brown, 2002). A subsample (1 L bottle or 348 cm^3 soil can) of sediment was taken with every bucket weighed unless the sediment appeared to have the same texture, moisture content, and organic matter, in which case every other bucket was subsampled. The sample bottles and soil cans were tightly capped in the field and taken to the laboratory for further processing. The samples were weighed for wet mass in the laboratory, then oven dried at 55°C to a stable dry mass and reweighed. The total mass of water in each bottle and soil can was then determined as the difference of the wet and dry masses, and the quantified water and sediment percentages for the respective samples were used to determine the water and dry sediment masses for the associated field bucket samples. All sediment values reported for silt fences are based on the derived dry sediment masses.

Vegetation, ground cover, and surface measurements

Short-hillslope plots

Vegetation, ground cover, soil water repellency, and ground surface roughness were assessed for each of the two short-hillslope plots in each silt fence block. To minimize disturbance to these smaller silt fence plots, a single 4 m long × 2 m wide plot (short-hillslope characterization plot; Figure 5) was randomly selected and monumented for repeat sampling in an area immediately adjacent to each of the short-hillslope silt fence plots. For each short-hillslope characterization plot, foliar and ground cover were measured using the line-point intercept method (Pierson et al., 2010). Foliar and ground cover by life form were recorded for 20 points (20 cm spacing), along each of nine transects, spaced 20 cm apart and oriented perpendicular to the hillslope contour (180 points per plot). Percent cover by cover type for each plot was determined from the number of point contacts or hits for each respective cover type divided by the total number of points sampled. The relative ground surface height at each line-point sample location was derived as the distance between the ground surface and a survey transit level-line above the respective sample point (Pierson et al., 2010). A ground surface roughness for each short-hillslope characterization plot was calculated as the average of standard deviations of relative ground surface heights measured across the respective plot line-point transects (Pierson et al., 2010).

Soil water repellency at 0–5 cm depth was measured within each short-hillslope characterization plot (Figure 5) along one of the 4 m line-point vegetation transects. A single transect was randomly selected within each site characterization plot and was sampled for soil water repellency at 40 cm increments downslope (11 points) using the water drop penetration time (WDPT) procedure (DeBano, 1981). At each sampling point, three water drops were placed on the mineral soil surface (ash and litter removed) and the time required for each water drop to infiltrate was recorded (up to a maximum of 300 s). Following this procedure, 1 cm of soil was excavated and the procedure was repeated with three more drops. WDPT sampling iterations continued to a soil depth of 5 cm. Mean soil water repellency at each 1 cm depth (0, 1, 2, 3, 4, and 5 cm depths) for each sampled plot was determined as the mean of the three WDPT (s) samples for the respective depth. The mean soil water repellency across all sampled soil depths on each plot was derived as the average of the respective WDPT means for 0, 1, 2, 3, 4 and 5 cm soil depths. Soils were classified as wettable when WDPT was less than 5 s, slightly water repellent when WDPT ranged from 5 to 60 s, and strongly water repellent when WDPT was greater than 60 s (Bisdom et al., 1993). Soil water repellency sampling was limited to north-facing hillslopes during the 2015 field campaign due to autumn rainfall events, but was sampled on both north- and south-facing aspects in summer 2016 and 2017.

Long-hillslope and swale plots

Vegetation foliar and ground cover for each long hillslope and swale plot (Figure 5) was quantified using line-point intercept methods (Herrick et al., 2017) along four 30 m transects. Transect locations for each long hillslope and swale plot were determined by dividing the upslope distance from the respective silt fence to the top of the hillslope topographic break into four evenly spaced sections. A single transect was established spanning each section, oriented parallel to the hillslope contour. These transects were installed and sampled to capture the variability in cover from the base of each long hillslope and swale plot to the top of the hillslope. Foliar and ground cover by lifeform were measured at 0.5 m increments along each 30 m transect (61 points per transect). Percent cover by cover type for each transect was determined from the number of point contacts or hits for each respective cover type divided by the total number of points sampled (Pierson et al., 2010). Percent cover by cover type for each hillslope and swale plot was determined as the average of respective measures across each of the four transects in the plot.

Statistical analyses

All statistical analyses were performed using SAS software, version 9.4 (SAS Institute Inc., 2013). Statistical analyses of silt fence sediment values, foliar and ground cover variables, and WDPT data were conducted using a mixed model procedure (Proc Mixed) in SAS (Littell et al., 2006). Mean separation analyses of foliar and ground cover and WDPT data for short-hillslope characterization plots applied a mixed model with two aspects (north and south) and three treatment years (2015, 2016, and 2017). Mean separation analyses of silt fence sediment and foliar and ground cover data on long-hillslope and swale silt fence plots applied a mixed model with two aspects (north and south) and two treatment years (2016 and 2017). Normality of data was evaluated prior to analysis of variance using residual plots and the Shapiro–Wilk test, and deviance from normality was addressed by data transformation. Back-transformed means are reported. Mean separation was determined using the LSMEANS statement (SAS Institute Inc., 2013). All reported significant effects were tested at the $p < 0.05$ level.

Results

Fire impacts on vegetation, ground cover, and surface conditions

Initial post-fire vegetation and ground surface conditions

Initial cover and ground surface conditions in the first few months following the Soda Fire were measured solely on the

short-hillslope characterization plots. The fire consumed nearly all live above-ground vegetation (Table I), leaving 0–5% total foliar cover across both north- and south-facing hillslopes. Total foliar cover in autumn 2015 consisted mainly of burned shrub skeletons. The ground surface in this immediate post-fire period was mostly bare (62–66% ash, bare soil, and rock) (Table I). North-facing slopes had a higher percentage of ash cover (49%) and less rock cover (2%) than the south-facing slopes (23% ash cover, 31% rock cover), and bare soil averaged 9–15% across all plots. The greater ash cover on north-facing hillslopes likely reflects a greater pre-fire vegetation cover on that aspect and therefore a greater burn severity and sediment availability, at least in patches, relative to the south-facing hillslopes (e.g., Figure 3). A lesser burn severity on the south-facing aspects is further implicated by the greater remaining litter cover (36% cover) on that aspect relative to the north-aspect plots (15% cover) immediately post fire (Table I). Soils on the north-facing aspect were water repellent from 0 to 5 cm soil depth and were strongly water repellent at 1–4 cm soil depths (Figure 7). Although soil water repellency was not systematically quantified on south-facing slopes in autumn 2015, randomly located WDPT tests on south-facing slopes during field reconnaissance immediately post fire indicated the presence of soil water repellency throughout the watershed. Ground surface roughness averaged 35–41 mm across north- and south-aspect plots in the immediate post-fire period (Table I).

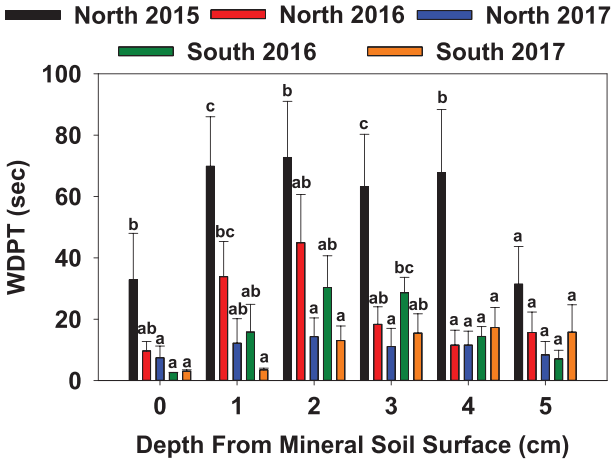

Figure 7. Soil water repellency presence and strength (persistence) as measured by the water drop penetration time (WDPT) tests on north-facing (North) and south-facing (South) hillslopes in the Murphy Creek Experimental Watershed the autumn immediately after the Soda Fire (2015) and in the summer season 1 year post fire (2016) and 2 years post fire (2017). Soils were considered wettable when WDPT was <5 s, slightly water repellent if WDPT ranged from 5 s to 60 s, and strongly water repellent if WDPT > 60 s (Bisdom et al., 1993). Error bars depict standard error. Means at a depth (0, 1, 2, 3, 4, or 5 cm) across aspects and years followed by different lower-case letters are statistically different ($p < 0.05$).

Changes in vegetation, ground cover, and surface conditions

Short-hillslope plots. Total foliar cover increased substantially across north- and south-aspect plots from autumn 2015 to summer 2016, the first growing season post fire (Table I). Total foliar cover increased more than 130-fold (91% cover) on the north-facing hillslopes over one growing season, owing primarily to increases in forb cover (69%) and grass cover (21% cover). Total foliar cover on south-facing hillslopes approached 60% and, as on north aspects, was mainly forbs (46% cover) and grasses (10% cover). Litter cover declined (to 4–6%) across both aspects over the first year post fire, and total bare ground (mostly bare soil and rock) exceeded 80%, on average, across all short-hillslope plots by summer 2016 (Table I). Soil water repellency persisted at all depths on north aspects in summer 2016, but was generally lesser (slight) for most depths relative to respective measures immediately post fire (Figure 7). Soil water repellency was present (slight) at all depths on south-facing slopes in the first summer post fire (Figure 7). The strength of soil water repellency was generally greatest at 1–2 cm soil depths on north aspects and 2–3 cm soil depths on south aspects (Figure 7). Ground surface roughness averaged 39–50 mm across plots on north and south aspects after the first growing season (Table I).

After two growing seasons, total foliar cover approached or exceeded 100% and ground cover was similar to immediate post-fire levels across both aspects (Table I). High forb (71%) and grass (65%) cover contributed to a total foliar cover of 140% on north-facing hillslopes in summer 2017. Total foliar cover on south-facing hillslopes approached 100% in summer 2017 and likewise comprised of mostly forbs (51% cover) and grasses (44% cover). Litter recruitment over the second growing season reduced bare ground by about 1.5-fold across both aspects relative to the previous summer (Table I). By summer 2017, total ground cover was 48% on north-facing hillslopes and 36% on south-facing hillslopes, and litter cover averaged 45% on north-aspect and 35% on south-aspect plots. Soil water repellency was present at all depths on north-facing and south-facing hillslopes 2 years post fire (Figure 7), but, for depths with the strongest repellency, the strength of repellency was reduced by half relative to measures in summer 2016. Two growing seasons post fire, ground surface roughness averaged 47 mm on north-aspect plots and 64 mm on south-aspect plots, and was not significantly different from respective measures of the immediate post-fire conditions in autumn 2015.

Table I. Foliar and ground cover and ground surface roughness measured on short-hillslope characterization plots (8 m^2) on north-facing (North) and south-facing (South) hillslopes in the Murphy Creek Experimental Watershed during the first autumn post fire (2015) and in summers during the first (2016) and second (2017) years post fire

Short-hillslope characterization plots						
	North			South		
	2015	2016	2017	2015	2016	2017
Foliar cover variables (%)						
Total	0.7a	91.2c	139.6d	5.2a	57.0b	98.5c
Shrub	0.0a	0.0a	0.2a	0.0a	0.2a	1.9a
Grass	0.0a	21.3b	64.9d	0.3a	10.1b	44.3c
Forb	0.0a	69.0c	70.6c	0.9a	45.8b	50.8b
Ground cover (%) and surface roughness						
Total ground[a]	34.0b	16.4a	47.5b	37.9b	10.8a	36.3b
Basal plant	19.1c	8.5b	2.5a	1.6a	5.6ab	0.3a
Litter	14.9a	6.3a	44.5b	36.3b	4.1a	35.4b
Ash[b]	49.4	0.0	0.0	22.8	0.0	0.0
Bare soil	14.6a	79.0d	45.2b	8.7a	68.8 cd	55.6BC
Rock	2.0a	4.6a	7.2a	30.5c	20.4b	8.0a
Bare ground[c]	66.0a	83.6b	52.5a	62.1a	89.2b	63.7a
Average surface roughness (mm)	35a	39a	47ab	41ab	50ab	64b

[a]Total ground cover is a total of basal plant, litter, moss, standing dead, and woody dead ground cover.
[b]Excluded from statistical analyses.
[c]Bare ground is total percentage of ash, bare soil, and rock cover.
Means within a row followed by a different lower-case letter are significantly different ($p < 0.05$).

Long-hillslope plots and swales. Similar to recovery on the short-hillslope plots, foliar and ground cover changes on long-hillslope and swale plots during the first few years post fire were largely increases in forb and grass foliar cover and litter ground cover (Table II). Trends in the amounts of foliar and ground cover for most cover variables were similar across long-hillslope and swale plots by aspect in each study year. In the first summer post fire, total foliar cover on north-facing long-hillslope and swale plots averaged near 85% and comprised near 50% forb cover and about 30% grass cover. Bare ground and litter cover averaged near 85% and 5%, respectively, across the same plots in summer 2016. Total foliar cover on south-facing long-hillslope and swale plots averaged about 105% and was near 35% forb cover and about 70% grass cover. As with the short-hillslope plots, rock cover was generally greater on south-facing hillslopes (Table II). Bare ground and litter cover averaged about 80% and 10%, respectively, across long-hillslope and swale plots on south-facing hillslopes in summer 2016. By the end of two growing seasons, total foliar cover was, on average, 117–139% across long-hillslope and swale plots on north- and south-facing hillslopes. Total foliar cover in summer 2017 consisted of approximately 60% forb cover and 70% grass cover on the north-facing hillslopes and swales, and approximately 40% forb cover and 80% grass cover on south-facing hillslopes and swales. Although substantial foliar cover recruitment occurred over the 2-year study, bare ground was, on average, 67–77% across all long-hillslope and swale plots in summer 2017 (Table II). In summer 2017, bare ground on north-aspect plots was mainly bare soil (65–69%) and on south-aspect plots was 47% bare soil and 21% rock. Litter cover increased by summer 2017 to about 23% across all plots on north-aspect and to more than 30% on south-aspect plots (Table II).

Water input and seasonality of streamflow and water-driven erosion processes

Watershed-scale processes

Water input as precipitation (Figure 8a) and outflow as streamflow (Figure 8c) throughout the study period are within historical ranges and trends for MCEW (Figure 9) and represent relatively dry and wet years the first (2016) and second (2017) years post fire, respectively. Historical records clearly show that water yield from MCEW is well correlated with precipitation input, and the 2016 and 2017 water years in this study are typical of that relationship (Figure 9). Precipitation input was approximately 415 mm for the 2016 water year and 649 mm for the wetter 2017 water year. Watershed-scale annual water yield in the same years was 144 mm and 304 mm, respectively, with water yield in 2017 more than double that of 2016. In both years, precipitation commonly occurred during the cool to cold seasons at or near-freezing conditions (Figures 8a and 8b) with snow cover or frozen to near-frozen surface soils. The rising limbs and peaks in streamflow on the hydrographs from the Murphy Creek Weir in 2016 and 2017 water years reflect these seasonal water inputs (Figure 8c). In both years, streamflow initially rose with wetting by cool autumn rainfall events and exhibited occasional spikes and a seasonal peak associated with cool- and cold-season water input by rainfall and snowmelt (Figure 8). In both water years, we observed extensive wind redistribution of snow into persistent drifts within hillslope hollows and swales (Figures 10a and 10b), including those with silt fences. We did not instrument swales for streamflow measurement, but observed streamflow through swales coming from snowdrifts throughout the snowmelt season (Figure 10a). The observed seasonality of water input and surface conditions during water input clearly drives watershed-scale sediment yield at MCEW. As evident from cumulative sediment yield through the weir in water years 2016–2017 (Figure 8d), sediment delivery at the watershed scale increased sharply at the onset of cool-season runoff and occasionally spiked during cold-season rain-on-frozen soil, rain-on-snow, and snowmelt events (Figure 8). Streamflow and sediment delivery during the summer months (June to August) were negligible during the 2 years after the fire (Figures 8c and 8d), even with occasional summer rainstorm events. Collectively, the meteorological, streamflow, and sediment data clearly indicate that runoff and sediment delivery at MCEW during the study period were driven primarily by cool- and cold-season hydrologic processes, consistent with trends in the historical record (Figures 8 and 9).

Table II. Foliar and ground cover measured on long-hillslope and swale silt fence plots on north-facing (North) and south-facing (South) hillslopes in the Murphy Creek Experimental Watershed in summers during the first (2016) and second (2017) years post fire

	Long hillslopes				Swales			
	North		South		North		South	
	2016	2017	2016	2017	2016	2017	2016	2017
Foliar cover (%)								
Total	84.3a	138.5c	99.2ab	117.1BC	82.5a	129.2b	110.7ab	121.3b
Shrub	2.6a	8.3a	0.0a	0.8a	1.4a	1.2a	0.5a	2.0a
Grass	28.1a	67.5b	61.7b	77.5b	28.8a	68.5b	75.8b	80.5b
Forb	51.8b	57.8b	36.3a	37.8a	52.0b	56.1b	33.2a	37.7a
Ground cover (%)								
Total ground[a]	12.7a	31.1a	14.6a	31.3a	17.8a	23.4a	20.8a	32.8a
Basal plant	7.7b	4.0b	5.2b	0.4a	10.1c	3.8b	10.5c	0.4a
Litter	3.7a	26.2BC	9.2ab	30.7c	7.0a	19.4ab	9.8a	32.2b
Ash[b]	0.0	0.0	0.0	0.0	0.0	0.0	0.0	0.0
Bare soil	79.5b	65.3ab	52.7a	44.9a	68.4a	69.3a	55.9a	48.8a
Rock	7.8a	3.6a	32.7b	23.8b	17.2b	7.4a	23.4b	18.4b
Bare ground[c]	87.3a	68.9a	85.4a	68.7a	85.7a	76.6a	79.2a	67.2a

[a]Total ground cover is the total of basal plant, litter, moss, standing dead, and woody dead ground cover.
[b]Excluded from statistical analyses.
[c]Bare ground is total percentage of ash, bare soil, and rock cover.
Means within a row by plot type (long hillslopes or swales) followed by a different lower-case letter are significantly different ($p < 0.05$).

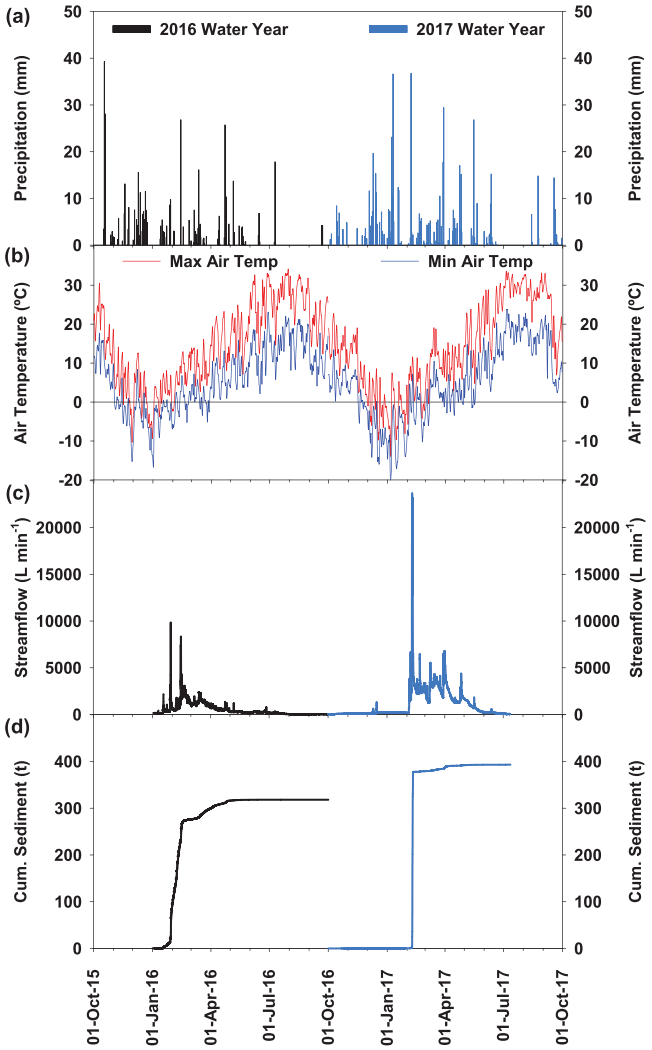

Figure 8. Measured and derived daily precipitation (a), minimum and maximum air temperatures (b), watershed-scale streamflow (c), and watershed-scale cumulative sediment delivery (d) at the Murphy Creek Experimental Watershed for the 2016 water year (1 October 2015 to 30 September 2016) and 2017 water year (1 October 2016 to 30 September 2017) following the 2015 Soda Fire. Streamflow (c) and sediment (d) are based on respective measures at the Murphy Creek Weir. Data from US Department of Agriculture, Agricultural Research Service, Northwest Watershed Research Center (USDA-ARS, 2015, 2016, 2017).

Silt fence plot-scale processes

Water year 2016: first year post fire. Sediment delivery to silt fence plots exhibited some variability between aspects (Table III), but was well synchronized with timing of watershed-scale streamflow (Figures 8c and 8d). Based on data from the nearby Whiskey Mountain Station, several minor (<5 mm) precipitation events occurred in MCEW during the silt fence installation period immediately after the fire. However, we observed no signs of erosion in the field and observed no streamflow during that time. Trace amounts of fine sediment and organic debris were observed in a few north-aspect silt fences on 15 October 2015, and these unquantified amounts were attributed to aeolian processes. All silt fence installations were complete on the north-facing hillslopes before the first large rainfall event on 18 October 2015 (>30 mm; Figure 8a). Field reconnaissance after the storm found no sediment in the completed north slope fences. Daily minimum and maximum air temperatures dropped substantially during November 2015, and both measures approached freezing by late November 2015 (Figure 8b). Several precipitation events (6–14 mm) occurred in MCEW from 18 to 24 November 2015 at and near freezing air temperatures (Figures 8a and 8b). Soil temperature data from Whiskey Mountain Station and Johnson Draw Station, at similar elevations to MCEW, indicate that surface soils were

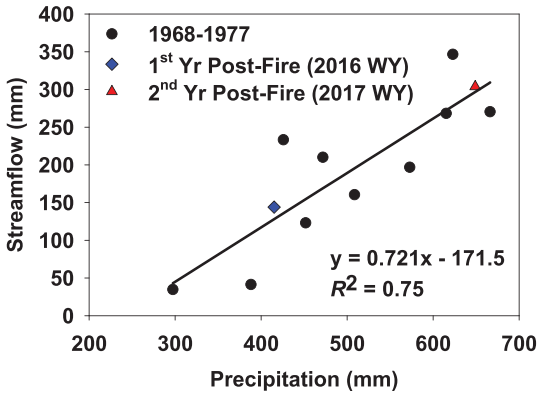

Figure 9. Annual streamflow (mm) and precipitation (mm) measured at the Murphy Creek Experimental Watershed as reported in the US Department of Agriculture, Agricultural Research Service, Northwest Watershed Research Center (USDA-ARS-NWRC) long-term streamflow (Pierson et al., 2000, 2001a) and precipitation (Hanson, 2000, 2001) databases for the Reynolds Creek Experimental Watershed for years 1968–1977 and as reported in Vega (2018) for the 2016 water year (2016 WY; 1 October 2015 to 30 September 2016) and 2017 water year (2017 WY; 1 October 2016 to 30 September 2017) following the Soda Fire. Data for 2016 and 2017 water years available from USDA-ARS-NWRC (USDA-ARS-NWRC, 2015, 2016, 2017). [Colour figure can be viewed at wileyonlinelibrary.com]

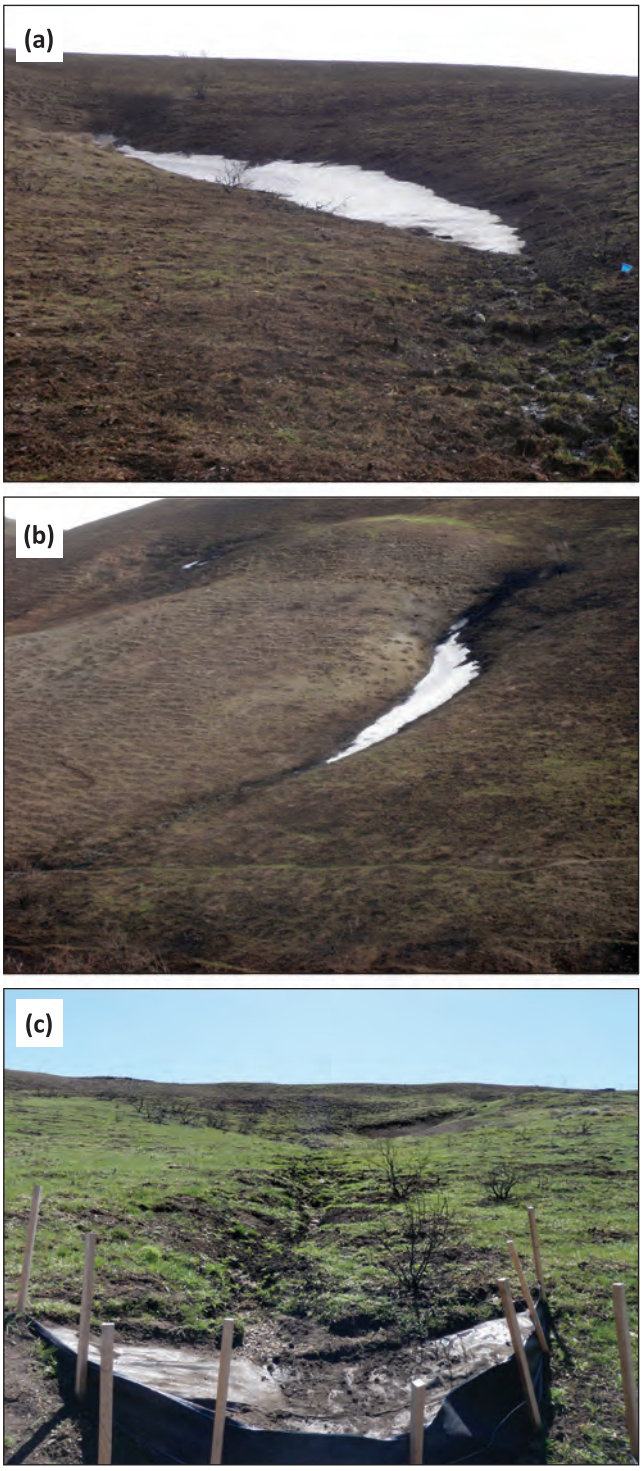

Figure 10. Photographs of snow drifts (a, b) and drift–snowmelt runoff in hillslope hollows or swales on north-facing hillslopes in the Murphy Creek Experimental Watershed in the first winter (2016) after the Soda Fire, and (c) upslope contributing area in a swale plot with incision following the snowmelt runoff period in May 2016, approximately 10 months post fire. Photos by US Department of Agriculture, Agricultural Research Service, Northwest Watershed Research Center. [Colour figure can be viewed at wileyonlinelibrary.com]

likely frozen on the north-facing hillslopes and near freezing on the south-facing hillslopes during these events (Vega, 2018). Field surveys on 24 November 2015 found sediment in nearly all fences on the north-facing hillslopes, substantial sediment in swale fences on north-facing hillslopes, and zero to a trace of sediment in silt fences throughout the blocks on the south-facing hillslopes. Field surveys on 30 November 2015 found snow and frozen sediment in all fences on the north aspect, frozen soil conditions throughout silt fence blocks on both aspects, and streamflow and ice at the Murphy Creek Weir. Numerous precipitation events occurred through the winter cold season (December 2015 to February 2016) inclusive of rainfall and snowfall (Figure 8), and culminating in a rise to peak flow in February 2016 (Figure 8c). Field surveys on 2–4 March 2016 found thawed sediment in all fences on the north-facing hillslopes, rilling through swales upslope of fences and downslope to the channel on the north aspect, and residual snow drifts and streamflow in swales on north-facing hillslopes throughout MCEW (Figure 10). Surveys on the same date found substantial sediment in swale fences on the south-facing hillslopes, but nearly all short- and long-hillslope plots on that aspect were devoid of sediment. The sediment observed in swales on the south-facing hillslopes on 2–4 March 2016 was likely the result of runoff from a 14 February 2016 precipitation event (27 mm), associated with rain on a shallow snowpack or frozen or saturated soils (Figure 8). The Murphy Creek Weir hydrograph and cumulative sediment curve show a spike in runoff and rise in sediment in mid-February (Figures 8c and 8d), which reflect this event. Field surveys on 1–8 April 2016 found no residual snow cover, streamflow discontinued in swales on north- and south-facing aspects, and persistent streamflow in the main channel and through the Murphy Creek Weir. All silt fences were routinely sampled and cleaned out during the March to April 2016 field surveys. Additional field surveys following spring and summer rainfall in May to September 2016 found only negligible amounts of sediment in various fences, indicating that nearly all the sediment delivered to silt fences during the first year post fire occurred due to runoff from frozen soils and snowmelt, associated with cold-season hydrologic processes.

Water year 2017: second year post fire. Similar to the first year, sediment delivery to silt fences in the second year post fire occurred solely during winter months. Approximately 46% (301 mm) of the precipitation in the 2017 water year occurred in the first few months of winter. The majority of sediment delivered to silt fences (Table III) and the weir (Figure 8d) in the second year occurred due to runoff through swales on 7–9 February 2017 associated with rain-on-snow and subsequent snowmelt (Figure 8). Field surveys following the events found substantial sediment in all swales on the north-facing hillslopes and two swales on the south aspect, and negligible to minor sediment delivery to nearly all short- and long-hillslope plots across both aspects. Although an additional 269 mm of precipitation occurred throughout the spring and summer seasons, only trace levels of additional sediment were delivered to silt fences and through the weir after the 7–9 February 2017 events.

Water-driven sediment delivery across spatial scales

Short-hillslope silt fence plots

Sediment delivery to the short-hillslope plots was generally low and exhibited high spatial variability between and within aspects in the first year post fire (Table III). Sediment yield measured in the short-hillslope plots in the first year (water year 2016) was nearly 10-fold greater for north-facing (8.62 t ha^{-1}) than south-facing (0.99 t ha^{-1}) hillslopes (Table III). However, the total sediment mass collected in short hillslopes ranged from 0.00 to 0.10 t across both aspects in the first year post fire. Nearly all the short-hillslope silt fences on the north aspect received sediment (0.34–28.74 t ha^{-1}) in water year 2016, but only two of six short-hillslope fences received sediment on the south aspect (0.00–3.23 t ha^{-1}) that

Table III. Contributing areas and annual sediment values measured for short-hillslope, long-hillslope, and swale silt fence plots on north-facing and south-facing hillslopes in the Murphy Creek Experimental Watershed in summers the first (2016) and second (2017) years post fire

		North-facing hillslopes						South-facing hillslopes			
		2016		2017			2016		2017		
Plot ID	Area (ha)	Total sediment (t)	Sediment yield (t ha^{-1})	Total sediment (t)	Sediment yield (t ha^{-1})	Plot ID	Area (ha)	Total sediment (t)	Sediment yield (t ha^{-1})	Total sediment (t)	Sediment yield (t ha^{-1})
Short-hillslope sediment											
B1NS-1	0.003	0.007	2.327	0.000	0.000	B1SS-1	0.004	0.000	0.000	0.000	0.000
B1NS-2	0.003	0.002	0.697	0.000	0.000	B1SS-2	0.004	0.000	0.000	0.000	0.000
B2NS-1	0.004	0.001	0.338	0.000	0.000	B2SS-1	0.003	0.000	0.000	0.002	0.592
B2NS-2	0.003	0.054	17.243	0.000	0.000	B2SS-2	0.003	0.000	0.000	0.000	0.000
B3NS-1	0.003	0.095	28.742	0.000	0.000	B3SS-1	0.003	0.011	3.232	0.000	0.000
B3NS-2	0.003	0.008	2.360	0.001	0.211	B3SS-2	0.005	0.013	2.729	0.000	0.000
Mean	0.003	0.028b	8.618b	0.000a	0.035a	Mean	0.004	0.004a	0.993a	0.000a	0.099a
Long-hillslope sediment											
B1NB	0.088	0.232	2.630	0.000	0.000	B1SB	0.062	0.000	0.000	0.000	0.000
B2NB	0.016	0.015	0.938	0.000	0.000	B2SB	0.460	0.000	0.000	0.000	0.000
B3NB	0.132	0.182	1.379	0.008	0.060	B3SB	0.313	0.016	0.052	0.015	0.047
Mean	0.079	0.143b	1.649b	0.003a	0.020a	Mean	0.278	0.005a	0.017a	0.005a	0.016a
Swale sediment											
B1NSW	1.008	0.148	0.147	0.954	0.946	B1SSW	0.654	0.010	0.010	0.010	0.015
B2NSW	0.803	0.867	1.080	0.230	0.286	B2SSW	2.332	0.179	0.322	0.322	0.077
B3NSW	0.753	0.679	0.902	0.455	0.605	B3SSW	3.415	2.101	0.373	0.373	0.615
Mean	0.855	0.565a	0.709a	0.546a	0.612a	Mean	2.134	0.677a	0.235a	0.763a	0.236a

Means reported by variable type (Total sediment or Sediment yield) within a row followed by a different lower-case letter are significantly different ($p < 0.05$).

year. Sediment yield at the short-hillslope scale was minimal (0.04–0.10 t ha^{-1} on average) across both aspects in water year 2017, the second year post fire (Table III). Only one short-hillslope fence on each aspect received sediment over the second year, and total sediment yield to those plots was <0.01 t (Table III).

Long-hillslope silt fence plots

Sediment yield to long-hillslope plots was greater for the north-facing (1.65 t ha^{-1}) than south-facing (0.02 t ha^{-1}) aspects the first year post fire, and, for north-aspect plots, total sediment was substantially greater than measured at the short-hillslope scale in year 1 (Table III). All plots on the north-facing hillslopes received sediment (0.02–0.23 t) the first year post fire and only one plot on the south-facing hillslopes received sediment (0.02 t, in block 3) that year. Sediment yields for long-hillslope plots averaged about 0.02 t ha^{-1} on both aspects for the second year, but sediment delivery in the second year was limited to one long-hillslope plot on each aspect, ~0.01 t in each case (Table III).

Swale silt fence plots

Substantially more sediment was delivered to silt fences in swales (0.55–0.76 t on average) relative to the same measures in short (<0.01–0.03 t, on average) and long hillslopes (<0.01–0.14 t, on average) in each year (Table III). Sediment yields in the first year averaged 0.71 t ha^{-1} for swale fences on north-facing hillslopes and 0.24 t ha^{-1} for swale fences on the south-facing hillslopes. Total sediment delivered to swale silt fence plots in year 1 ranged 0.15–0.87 t on north-facing and 0.01–2.10 t on south-facing hillslopes. Sediment yield in swale plots in the second year remained high, on average (0.24–0.61 t ha^{-1}), and similar to levels measured during the first year (Table III). All swale fences on the north-facing aspect received substantial sediment (0.23–0.95 t) in year 2, but most (92%) of the total sediment collected in south-facing swale fences in year 2 was from one fence (2.10 t, B3SSW in block 3). We observed that much of the sediment delivered to that plot was associated with a head cut adjacent to a spring upslope of that fence within the swale. Regardless, the bulk (85–99%) of the sediment collected in silt fences over the first 2 years post fire (4.36 and 3.95 t) was from the swale plots across both aspects (Table III). The higher sediment loads in swale plots each year (Table III) are attributed to cold-season runoff flushing of fine sediments preferentially loaded into swales by observed aeolian processes in the immediate post-fire period.

Watershed-scale sediment delivery and controls and drivers

In contrast to measured streamflow (Figure 8c), sediment yield through the Murphy Creek Weir was similar in the first (2.47 t ha^{-1}) and second (3.05 t ha^{-1}) years after fire (Figure 11). The similarities in sediment yield across the 2 years with substantially different streamflow are attributed to changes in sediment availability, vegetation conditions, and ground cover over the 2-year period. Sediment concentrations at the weir were linearly correlated with measured streamflow in both years and declined by the second year post fire for most levels of streamflow (Figure 12). Likewise, sediment yields for silt fence plots generally declined with decreasing bare ground over the 2-year study (Figure 13). In both years, the majority of sediment measured at the weir was discharged by runoff from cold-season hydrologic processes, inclusive of rainfall on frozen soils, a shallow snowpack, or saturated soils and from snowmelt. Each year of the study, sediment discharged through the weir (Figure 8d) increased substantially in the first few months of winter and then gradually increased throughout

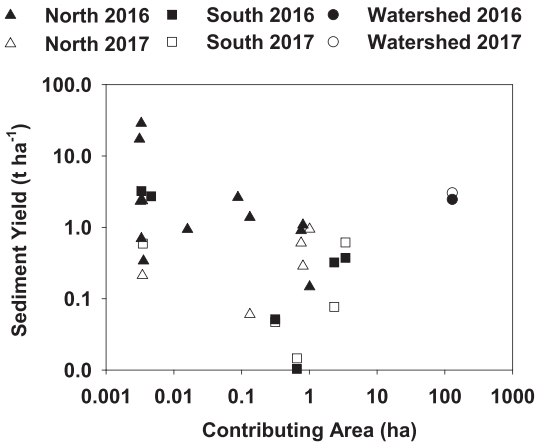

Figure 11. Sediment yield measured in silt fences on north-facing (North) and south-facing (South) hillslopes/swales and at the Murphy Creek Weir (Watershed) in the Murphy Creek Experimental Watershed plotted versus contributing area for the 2016 water year (1 October 2015 to 30 September 2016) and 2017 water year (1 October 2016 to 30 September 2017) following the Soda Fire. Sediment yield at the Murphy Creek Weir for 2016 and 2017 water years available from USDA-ARS-NWRC (USDA-ARS-NWRC, 2015, 2016, 2017).

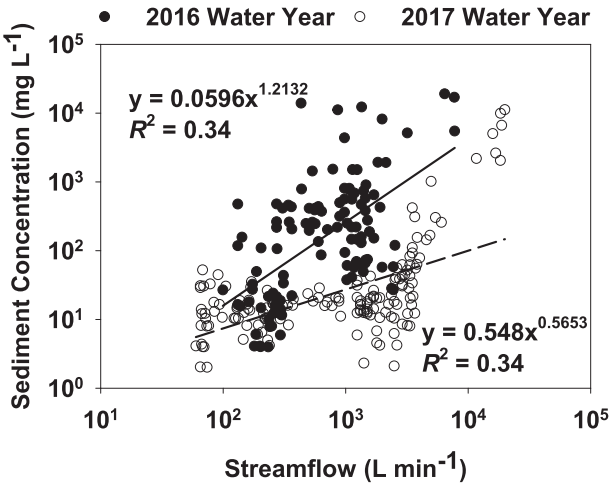

Figure 12. Relationship between sediment concentrations and streamflow at the Murphy Creek Weir for the 2016 water year (1 October 2015 to 30 September 2016) and 2017 water year (1 October 2016 to 30 September 2017) following the 2015 Soda Fire. Data available from USDA-ARS-NWRC (USDA-ARS-NWRC, 2015, 2016, 2017).

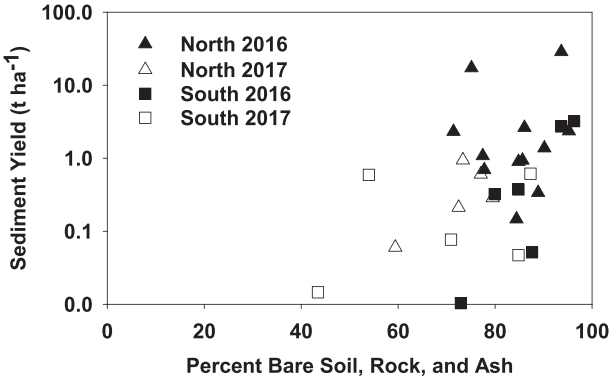

Figure 13. Annual sediment yield plotted versus percent bare ground as measured on silt fence plots on north-facing (North) and south-facing (South) hillslopes in the Murphy Creek Experimental Watershed in the first (2016) and second (2017) years following the 2015 Soda Fire.

much of the cold season. Sediment discharge through the weir was negligible during the late spring and summer months.

Discussion

Wind and cold-season water process interaction

The chronological sequence of sediment delivery over a 2-year period during this study suggests that the interaction of aeolian and cold-season hydrologic processes can be a key driver of post-fire erosion rates in sagebrush steppe rangelands. We anticipated that first- and second-year hillslope erosion rates would be mainly driven by rainsplash and overland flow processes during high-intensity summer thunderstorm events (Pierson et al., 2001b, 2002, 2008a, 2009, 2011; Williams et al., 2014a, 2016b). Pierson et al. (2002) describe such an event for burned sagebrush rangelands in the Boise Front Range, near Boise, Idaho, approximately 75 km from research sites in this study. As described in that report, a 9 min summer thunderstorm with an average intensity of 67 mm h^{-1} caused extensive flooding and mudflows from sloping sagebrush hillslopes with burned water-repellent surface soils. Meyer et al. (2001) chronicle similar hydrologic and erosion responses from burned hillslopes in dry forests of southwestern Idaho. An intense summer thunderstorm at a burned site in that study generated extensive runoff, rilling, gullying, and debris flows. Such responses to intense rainfall on burned rangelands and dry forests are well documented in the literature (see Robichaud, 2009; Moody et al., 2013; Williams et al., 2014a). Cannon et al. (1998) describe a network of extensive hyperconcentrated flows and debris flows from burned dry forest and rangeland hillslopes in complex topography that occurred during torrential rainfall events several months following wildfire. The authors found that wind redistribution of surface soils following burning contributed substantially to loading of side channels with loose sediments. This material combined with existing sediments and overland flow during intense rainfall that inundated a 14 ha area with 70 000 m^3 of sediment. We observed less extreme but similar flushing of wind-deposited sediments from burned hillslope hollows and swales in this study. However, in our case, the flushing was mainly by runoff from prolonged cold-season hydrologic processes. High levels of erosion and redistribution of sediment by aeolian processes are common following wildfire in sagebrush steppe (Sankey et al., 2009a, 2012a; Wagenbrenner et al., 2013), and complex topography in these systems affects snow distribution and retention and the generation and concentration of streamflow (Flerchinger and Cooley, 2000; Chauvin et al., 2011; Kormos et al., 2017). We observed substantial wind-driven redistribution of sediment into swales in the immediate post-fire period (Figure 4) and flushing of portions of these sediments into swale silt fences by runoff (Figure 6b) associated with cold-season hydrologic and erosion processes typical of snow-dominated sagebrush uplands (Blackburn et al., 1990; Pierson and Wight, 1991; Seyfried and Wilcox, 1995; Flerchinger and Cooley, 2000; Pierson et al., 2000, 2001a; McNamara et al., 2005; Seyfried et al., 2009; Williams et al., 2009). The flushing of sediment from swales is specifically attributed to the runoff from early-winter rain-on-snow and rain-on-frozen soil events and subsequent runoff from melting of snowdrifts formed within swales (Figure 8), through wind redistribution of snow (Figure 10; Winstral et al., 2013). The lack of summer season sediment delivery in this study does not negate the fact that sediment was available, but rather reflects that summer-season water input during the study was less than that necessary to generate substantial overland flow (Pierson et al., 2011; Williams et al., 2014a). The high levels of sediment delivered in our study in association with interacting wind and over-winter hydrologic processes suggest that these systems can be vulnerable to erosion for a prolonged period and that cold-season runoff is capable of transporting substantial sediment loads from hillslopes and swales in the absence of summer-season thunderstorms (McGuire et al., 2016). These sediment loads may pose hazards for instream values-at-risk such as water quality or aquatic habitat and, if stored on site, can serve as a source for downstream sediment pulses during subsequent channel-flushing events (Cannon et al., 1998, 2001; Minshall et al., 2001; Meyer and Pierce, 2003; Pierce et al., 2004; Robichaud et al., 2013a). This has implications for post-fire hydrologic and erosion risk assessment and modeling, which often focus on the likelihood for the more commonly reported responses to short-duration, high-intensity summer thunderstorm events (Benavides-Solorio and MacDonald, 2005; Pierson et al., 2011; Moody et al., 2013; Williams et al., 2014a).

Spatial scaling of post-fire erosion processes and sediment delivery

Differences in sediment delivery across spatial scales in this study (Table III) reflect the availability of sediment post-fire and connectedness of runoff and erosion processes (Robichaud et al., 2013a; Williams et al., 2014b, 2016a). In the first year post fire, sediment delivery per unit area for silt fence plots generally declined with increasing contributing area (Figure 11), whereas total sediment delivered increased with increasing plot contributing area (Table III). For undisturbed sagebrush rangelands, erosion generally decreases with increasing plot area due to limited connectivity of runoff and sediment sources and deposition near roughness elements that disrupt runoff and erosion processes (Pierson et al., 1994b, 2009). Burning generally increases sediment availability and connectivity of runoff and erosion processes in the first year post fire (Shakesby and Doerr, 2006; Spigel and Robichaud, 2007; Pierson et al., 2009, 2011; Moody et al., 2013; Williams et al., 2014a, 2014b, 2016a). Further, this connectivity of sediment sources and physical processes immediately post fire is enhanced with increasing water input, i.e., increasing rainfall intensity (Benavides-Solorio and MacDonald, 2005; Pierson et al., 2011; Robichaud et al., 2013b; Williams et al., 2016a). We attribute the decreasing sediment yield with increasing contributing area in the first year of this study to poorly connected runoff and erosion processes across spatial scales associated with the limited water input rates of prolonged cool-season precipitation and snowmelt. Measured unit-area sediment yields the first year post fire across the short- and long-hillslope plots suggest that much of the sediment detached over small areas was subsequently deposited and stored along hillslopes, consistent with patterns of sediment transport and deposition on undisturbed sagebrush hillslopes (Pierson et al., 1994b, 2009). Although sediment yields per unit area were generally lower for swale plots than short- and long-hillslope plots, sediment delivery from swales was mainly associated with flushing of stored sediments along drainage lines and immediately adjacent side slopes (Benavides-Solorio and MacDonald, 2005; Robichaud et al., 2013a), with potentially very limited contribution from disconnected areas on higher side slopes. Still, the ample sediment availability and the high sediment transport capacity of concentrated overland flow within swales resulted in swale plots receiving the most total sediment the first year post fire (Table III). We observed incision along the main flow

paths draining into all of our silt fences within swale plots (Figure 10c), indicating enough flow energy for detachment and transport along drainage lines. The ample fine sediments transported through swales during the first year post fire contributed to higher sediment concentrations in streamflow in the first year relative to the second, even though streamflow was greater during the second year (Figure 12). By 2017, sediment yield for short- and long-hillslope plots (Table III) was limited, likely due to reduced sediment availability along hillslopes and perhaps also to poor hillslope runoff and erosion process connectivity in lieu of increased cover (Tables I and II; Al-Hamdan et al., 2013; Benavides-Solorio and MacDonald, 2005; Pierson et al., 2009; Robichaud et al., 2013a). In contrast to short- and long-hillslope plots, total sediment and sediment per unit area were similar across years for swale plots and were generally greater for swale plots on the north aspect (Table III). Our field reconnaissance immediately post fire observed more substantial redistribution of sediment into swales on the north aspect than south aspect due to the prevailing wind direction. Likewise, we observed more frequent snowdrift formation and persistence in swales on the north aspect relative to the south aspect throughout the study. Further, greater rock cover (Tables I and II) on south-facing than north-facing aspects may also have limited sediment availability and transport on south-facing silt fence plots relative to those on north-facing hillslopes (Nearing et al., 1999; Shakesby, 2011). The high sediment yields from swale plots in the second year post fire contributed to similar watershed-scale sediment delivery across study years (Figure 11). High runoff in the second year suggests there was enough drift snowmelt within swales to flush residual sediment, but the reduced streamflow sediment concentrations that year imply a reduction in sediment availability.

Post-fire recovery, sediment availability, connectivity, and erosion magnitude

Field observations, aeolian and hydrologic processes interaction, and sediment yields measured in this study, highlight the challenges in determining post-fire hydrologic and erosion recovery and the potential magnitude of sediment delivery over the first few years post fire. Recovery of vegetation on sagebrush rangelands is initiated by increases in herbaceous cover to pre-fire levels in the first few years post fire and subsequent sagebrush re-establishment to pre-fire levels over the following 20 or more years, depending on site ecological attributes, fire severity, and post-fire climate trends (Harniss and Murray, 1973; Ziegenhagen and Miller, 2009; Miller et al., 2013). Recovery of ground cover amounts and distribution commonly takes longer and is highly variable (Miller et al., 2013). Field studies indicate that increases in runoff and erosion rates after fire on sagebrush rangelands often dissipate over the first 2–5 years post fire, but that amplified soil erodibility persists longer than fire-related increases in runoff generation (Pierson et al., 2008a, 2009, 2011; Williams et al., 2014a, 2016b). Decreased erosion in the first few years post fire then is usually associated with decreased runoff and transport capacity (Pierson et al., 2009; Williams et al., 2016b). These generalized recovery trends are largely based on plot-scale field studies of fire impacts on runoff and erosion under artificially applied rainfall at static high intensities (see Pierson and Williams, 2016). Therefore, these studies offer limited insight into post-fire recovery relative to runoff and erosion associated with cold-season hydrologic processes observed in this study. Certainly, recovery of vegetation to levels protective against high-intensity rainfall should reduce hydrologic and erosion vulnerability and offer ample protection against sediment transport by cold-season hydrologic processes (Williams et al., 2014a). However, assertion of recovery is potentially confounded at our study site by the wind redistribution of sediment to swales and the persistent dominance of cold-season runoff processes. At the conclusion of our summer 2017 field campaign, we observed incised flow paths in nearly all swales visited (e.g., Figure 10c) and the presence of ample residual fine sediment immediately adjacent to the flow paths. These observations suggest that sediment remains available in swales where runoff is likely to concentrate if a high-intensity rainfall event were to occur (Benavides-Solorio and MacDonald, 2005; Robichaud et al., 2013a). Further, bare ground exceeds 60% (Table II) and is above the threshold that limits runoff and soil erosion during high-intensity rainfall events on these rangelands (Pierson et al., 2008a, 2009). Reduced sediment concentrations in streamflow in the second year post fire suggest that the supply of available sediment has declined, but watershed sediment yield remains elevated over that of similar adjacent unburned sagebrush-dominated watersheds in the RCEW (Pierson et al., 2000, 2001a). Collectively, visible ample sediment in swales and persistent low ground cover and high watershed-scale sediment yield indicate that the study site remains susceptible to amplified erosion in swales during either a rare high-intensity summer rainfall event, long-duration rainfall on frozen or snow-covered soils, or over another year with high runoff from cold-season hydrologic processes (Benavides-Solorio and MacDonald, 2005; Kampf et al., 2016).

Sediment yields associated with combined aeolian and cold-season hydrology and erosion processes in this study are consistent with post-fire erosion levels documented in the literature (see Shakesby and Doerr, 2006; Moody and Martin, 2009; Shakesby, 2011). The mean sediment yields from silt fences in MCEW (Table III) are within the range of values most commonly reported for the first and second years post fire in bounded and unbounded plots (0.005–10 $t\,ha^{-1}\ yr^{-1}$) on rainfall- and snow-dominated sloping rangelands and forests in the USA (Benavides-Solorio and MacDonald, 2005; Robichaud et al., 2013b; Kampf et al., 2016) and the Mediterranean (frequently $<1\,t\,ha^{-1}\ yr^{-1}$, most $<10\,t\,ha^{-1}\ yr^{-1}$; Shakesby, 2011). The MCEW silt fence erosion rates are, however, lower than those reported in the literature for extreme rainfall events after wildfires and over the first few years post fire in regions with a high-intensity or monsoonal rainfall precipitation regime (10–200 $t\,ha^{-1}\ yr^{-1}$), such as the southwestern USA (Shakesby and Doerr, 2006; Moody and Martin, 2009; Shakesby, 2011). The lack of available pre-fire sediment yields for MCEW limits assessment of fire-induced increases in sediment yield over the first few years post fire. Sediment yields from similar adjacent and unburned sagebrush-dominated watersheds (3200–23 000 ha) in the greater RCEW range from 1.14 to 1.9 $t\,ha^{-1}\ yr^{-1}$ (Pierson et al., 2000, 2001a). Based on these data, first-year (2.47 $t\,ha^{-1}\ yr^{-1}$) and second-year (3.05 $t\,ha^{-1}\ yr^{-1}$) year sediment yields from MCEW were of the order of 1.3-fold to 2.7-fold greater than for unburned conditions, and represent substantial fire-induced increases in erosion driven by the interaction of wind and cold-season hydrologic processes. Post-fire MCEW catchment-scale sediment yields measured as suspended sediment are similar to those commonly reported from elsewhere in the USA (0.12–6.8 $t\,ha^{-1}\ yr^{-1}$; Moody and Martin, 2009) and the Mediterranean (0.036–5.7 $t\,ha^{-1}\ yr^{-1}$; Shakesby, 2011) in the first few years post fire, but the magnitudes of suspended sediment yields at MCEW relative to historical levels for adjacent unburned catchments suggest a lesser fire impact on catchment sediment delivery in our study relative to others in the literature, with 10- to 30-fold fire-induced increases not uncommon (Shakesby and Doerr, 2006).

Conclusions

Our study of a mountainous snow-dominated sagebrush site over a 2-year period post fire demonstrates that the interaction of aeolian processes and cold-season hydrology can be an important driver of erosion in complex terrain. We observed widespread redistribution of fine sediment by aeolian processes immediately following wildfire. Preferential loading of this material into swales provided a source for sediment delivery by runoff across spatial scales over the first 2 years post fire. Extensive bare conditions in the first year after fire facilitated high rates of erosion across short- and long-hillslope plots, in swales, and at the watershed scale. More than 85% of the total sediment collected in silt fences during the first year post fire was from swales and nearly all of it was delivered by runoff from rainfall on frozen soils or snow and during the seasonal melting of snowdrifts within swales. Sediment delivery in the second year declined across spatial scales for short- to long-hillslope plots, but was similar to first-year levels for swales and at the watershed scale. Effectively all sediment delivered to silt fences in the second year occurred from winter-season runoff within swales. The lack of sediment delivery during summer months was unexpected, but is attributed in part to limited summer thunderstorm activity during the study. Regardless, the results demonstrate that the interaction of wind- and cold-season hydrology-driven erosion is likely an important phenomenon on snow-dominated sagebrush uplands in complex topography. At our site, sediment yield at the watershed scale (2.47–3.05 $t\,ha^{-1}\ yr^{-1}$) was 1.3- to 2.7-fold greater than historical sediment yields from neighboring unburned watersheds. This suggests that interacting aeolian and cold-season hydrologic processes can contribute substantial loads of sediment to main-stem channels after fires. Ample residual sediment, extensive bare ground, and persistent high sediment yields at our site 2 years post fire indicate that recovery is ongoing and that the potential for higher than background levels of sediment delivery remains even after two growing seasons. Although our study is from one site, the observed widespread wind redistribution of sediment post fire, seasonality of runoff and erosion processes, and annual sediment yields are consistent with a substantial body of literature on burned snow-dominated sagebrush rangelands and dry forests. Our study is novel in that it provides measures of sediment transport associated with the interaction of wind- and water-driven erosion processes post fire. The consistency of observations and measured seasonal trends in post-fire erosion across this study and others from similar burned landscapes implies that responses over the 2-year period are not unique. We suggest that further quantification of the interacting effects of wind and cold-season hydrologic processes on post-fire erosion is paramount for advancing post-fire risk assessment and prediction for snow-dominated uplands. This need is particularly important for snow-dominated uplands where fire activity is increasing, such as sagebrush steppe.

Acknowledgements—Funding was provided by the Agricultural Research Service, US Department of Agriculture (USDA). The USDA is an equal opportunity provider and employer. Mention of a proprietary product does not constitute endorsement by USDA and does not imply its approval to the exclusion of the other products that may also be suitable. This work was also partially funded by the National Science Foundation, Reynolds Creek Critical Zone Observatory, Cooperative Agreement No. EAR-1331872. The authors thank Dr Patrick Clark (USDA Agricultural Research Service) for contributions of research support. We also thank Alex Boehm, Barry Caldwell, Zane Cram, Dr. Aaron Fellows, Tisha Ferris, Kyle Lindsay, Mark Murdock, and Nicholas Patton for contributions and/or logistical support to various components of the field data collection and laboratory and spatial analyses. Lastly, we are grateful for comments from multiple anonymous reviewers and the journal Editors, which aided revisions and improvements to this paper.

Conflict of interest

The authors declare no conflict of interest.

Data Availability Statement

Time series meteorological, streamflow, and sediment discharge data obtained and used in this study from the US Department of Agriculture (USDA), Agricultural Research Service (ARS), Northwest Watershed Research Center (NWRC), and Reynolds Creek Experimental Watershed instrumentation network are available by request from the USDA-ARS-NWRC; contact: Steven Van Vactor, USDA-ARS Hydrologist, steven.vanvactor@usda.gov.

References

Al-Hamdan OZ, Pierson FB, Nearing MA, Williams CJ, Stone JJ, Kormos PR, Boll J, Weltz MA. 2012. Concentrated flow erodibility for physically based erosion models: temporal variability in disturbed and undisturbed rangelands. *Water Resources Research* **48**(7): 1–15, Art No. W07504. https://doi.org/10.1029/2011WR011464

Al-Hamdan OZ, Pierson FB, Nearing MA, Williams CJ, Stone JJ, Kormos PR, Boll J, Weltz MA. 2013. Risk assessment of erosion from concentrated flow on rangelands using overland flow distribution and shear stress partitioning. *Transactions of the American Society for Agricultural and Biological Engineers* **56**(2): 539–548.

Balch JK, Bradley BA, D'Antonio CM, Gómez-Dans J. 2013. Introduced annual grass increases regional fire activity across the arid western USA (1980–2009). *Global Change Biology* **19**(1): 173–183.

Benavides-Solorio JDD, MacDonald LH. 2005. Measurement and prediction of post-fire erosion at the hillslope scale, Colorado Front Range. *International Journal of Wildland Fire* **14**(4): 457–474.

Bisdom EBA, Dekker LW, Schoute JFT. 1993. Water repellency of sieve fractions from sandy soils and relationships with organic material and soil structure. *Geoderma* **56**(1–4): 105–118.

Blackburn WH, Pierson FB, Seyfried MS. 1990. Spatial and temporal influence of soil frost on infiltration and erosion of sagebrush rangelands. *Water Resources Bulletin* **26**(6): 991–997.

Blackburn WH, Pierson FB, Hanson CL, Thurow TL, Hanson AL. 1992. Spatial and temporal influence of vegetation on surface soil factors in semiarid rangelands. *Transactions of the American Society of Agricultural Engineers* **35**(2): 479–486.

Cannon SH, Powers PS, Savage WZ. 1998. Fire-related hyperconcentrated and debris flows on Storm King Mountain, Glenwood Springs, Colorado, USA. *Environmental Geology* **35**(2–3): 210–218.

Cannon SH, Kirkham RM, Parise M. 2001. Wildfire-related debris-flow initiation processes, Storm King Mountain, Colorado. *Geomorphology* **39**(3–4): 171–188. https://doi.org/10.1016/s0169-555x(00)00108-2.

Cerdà A, Doerr SH. 2005. Influence of vegetation recovery on soil hydrology and erodibility following fire: an 11-year investigation. *International Journal of Wildland Fire* **14**(4): 423–437.

Chauvin GM, Flerchinger GN, Link TE, Marks D, Winstral AH, Seyfried MS. 2011. Long-term water balance and conceptual model of a semi-arid mountainous catchment. *Journal of Hydrology* **400**(1–2): 133–143. https://doi.org/10.1016/j.jhydrol.2011.01.031.

Davies KW, Bates JD. 2010. Vegetation characteristics of mountain and Wyoming big sagebrush plant communities in the Northern Great Basin. *Rangeland Ecology & Management* **63**(4): 461–466. https://doi.org/10.2111/rem-d-09-00055.1.

DeBano LF. 1981. *Water-repellent soils: a state of the art. General Technical Report PSW-GTR-46*. US Department of Agriculture, Forest Service: Berkeley, CA.

Edwards BL, Webb NP, Brown DP, Elias E, Peck DE, Pierson FB, Williams CJ, Herrick JE. 2019. Climate change impacts on wind and water erosion on US rangelands. *Journal of Soil and Water Conservation* **74**(4): 405–418.

ESRI. 2016. *ArcGIS Desktop: Release 10.4.1*. Environmental Systems Research Institute: Redlands, CA.

Flerchinger GN, Cooley KR. 2000. A ten-year water balance of a mountainous semi-arid Watershed. *Journal of Hydrology* **237**(1–2): 86–99.

Glenn NF, Finley CD. 2010. Fire and vegetation type effects on soil hydrophobicity and infiltration in the sagebrush-steppe. I. Field analysis. *Journal of Arid Environments* **74**(6): 653–659.

Godsey SE, Marks D, Kormos PR, Seyfried MS, Enslin CL, Winstral AH, McNamara JP, Link TE. 2018. Eleven years of mountain weather, snow, soil moisture and streamflow data from the rain–snow transition zone: the Johnston Draw catchment, Reynolds Creek Experimental Watershed and Critical Zone Observatory, USA. *Earth System Science Data* **10**(3): 1207–1216. https://doi.org/10.5194/essd-10-1207-2018.

Hanson CL. 2000. *Precipitation monitoring at the Reynolds Creek Experimental Watershed, Boise, Idaho, USA (ARS Technical Bulletin NWRC-2000-4)*. US Department of Agriculture, Agricultural Research Service, Northwest Watershed Research Center: Boise, ID.

Hanson CL. 2001. Long-term precipitation database, Reynolds Creek Experimental Watershed, Idaho, United States. *Water Resources Research* **37**(11): 2831–2834.

Harniss RO, Murray RB. 1973. 30 years of vegetal change following burning of sagebrush–grass range. *Journal of Range Management* **26**(5): 322–325.

Hasselquist NJ, Germino MJ, Sankey JB, Ingram LJ, Glenn NF. 2011. Aeolian nutrient fluxes following wildfire in sagebrush steppe: implications for soil carbon storage. *Biogeosciences* **8**(12): 3649–3659. https://doi.org/10.5194/bg-8-3649-2011.

Herrick JE, Van Zee JW, McCord SE, Courtright EM, Karl JW, Burkett LM. 2017. *Monitoring manual for grassland, shrubland, and savanna ecosystems*, 2nd edn. US Department of Agriculture, Agricultural Research Service, Jornada Experimental Range: Las Cruces, NM.

Hironaka MM, Fosberg M, Winward AH. 1983. *Sagebrush–grass habitat types of southern Idaho*, Bulletin 35. University of Idaho: Moscow, ID.

Ilangakoon N, Glenn NF, Spaete LP, Dashti H, Li A. 2016. 2014 lidar-derived 1 m digital elevation model data set for Reynolds Creek Experimental Watershed, southwestern Idaho. Data set. Boise State University, Boise Center Aerospace Laboratory, Boise, ID. doi: https://doi.org/10.18122/B26C7X

Johnson CW, Blackburn WH. 1989. Factors contributing to sagebrush rangeland soil loss. *Transactions of the American Society of Agricultural Engineers* **32**(1): 155–160.

Johnson CW, Gordon ND. 1988. Runoff and erosion from rainfall simulator plots on sagebrush rangeland. *Transactions of the American Society of Agricultural Engineers* **31**(2): 421–427.

Kampf SK, Brogan D, Schmeer S, MacDonald LH, Nelson PA. 2016. How do geomorphic effects of rainfall vary with storm type and spatial scale in a post-fire landscape? *Geomorphology* **273**(15): 39–51.

Kormos PR, Marks D, Pierson FB, Williams CJ, Hardegree SP, Havens S, Hedrick A, Bates JD, Svejcar TJ. 2017. Ecosystem water availability in juniper versus sagebrush snow-dominated rangelands. *Rangeland Ecology & Management* **70**(1): 116–128. https://doi.org/10.1016/j.rama.2016.05.003.

Kormos PR, Marks DG, Seyfried MS, Havens SC, Hedrick A, Lohse KA, Sandusky M, Kahl A, Garen D. 2018. 31 years of hourly spatially distributed air temperature, humidity, and precipitation amount and phase from Reynolds Critical Zone Observatory. *Earth System Science Data* **10**(2): 1197–1205. https://doi.org/10.5194/essd-10-1197-2018.

Littell RC, Milliken GA, Stroup WW, Wolfinger RD, Schabenberger O. 2006. *SAS for Mixed Models*. SAS Publishing: Cary, NC.

Marks D, Winstral A, Reba M, Pomeroy J, Kumar M. 2013. An evaluation of methods for determining during-storm precipitation phase and the rain/snow transition elevation at the surface in a mountain basin. *Advances in Water Resources* **55**: 98–110.

McGuire LA, Kean JW, Staley DM, Rengers FK, Wasklewicz TA. 2016. Constraining the relative importance of raindrop- and flow-driven sediment transport mechanisms in postwildfire environments and implications for recovery time scales. *Journal of Geophysical Research - Earth Surface* **121**(11): 2211–2237. https://doi.org/10.1002/2016JF003867.

McNamara JP, Chandler D, Seyfried M, Achet S. 2005. Soil moisture states, lateral flow, and streamflow generation in a semi-arid, snowmelt-driven catchment. *Hydrological Processes* **19**(20): 4023–4038.

McNamara JP, Benner SG, Poulos MJ, Pierce JL, Chandler DG, Kormos PR, Marshall H, Flores AN, Seyfried M, Glenn NF, Aishlin P. 2018. Form and function relationships revealed by long-term research in a semiarid mountain catchment. *WIREs Water* **5**(2): 1–14, e1267. https://doi.org/10.1002/wat2.1267.

Meyer GA, Pierce JL. 2003. Climatic controls on fire-induced sediment pulses in Yellowstone National Park and central Idaho: a long-term perspsective. *Forest Ecology and Management* **178**(1–2): 89–104.

Meyer GA, Pierce JL, Wood SH, Jull AJT. 2001. Fire, storms, and erosion events in the Idaho batholith. *Hydrological Processes* **15**(15): 3025–3038.

Miller RF, Knick ST, Pyke DA, Meinke CW, Hanser SE, Wisdom MJ, Hild AL. 2011. Characteristics of sagebrush habitats and limitations to long-term conservation. In *Greater Sage-Grouse: Ecology and Conservation of a Landscape Species and its Habitats. Studies in Avian Biology*, Knick ST, Connelly JW (eds), Vol. **38**. University of California Press: Berkeley, CA; 145–184.

Miller RF, Chambers JC, Pyke DA, Pierson FB, Williams CJ. 2013. *A review of fire effects on vegetation and soils in the Great Basin Region: response and ecological site characteristics*, General Technical Report RMRS-GTR-308. US Department of Agriculture, Forest Service, Rocky Mountain Research Center: Fort Collins, CO.

Minshall GW, Robinson CT, Lawrence DE, Andrews DA, Brock JT. 2001. Benthic macroinvertebrate assemblages in five central Idaho (USA) streams over a 10-year period following disturbance by wildfire. *International Journal of Wildland Fire* **10**(2): 201–213.

Moody JA, Martin DA. 2009. Synthesis of sediment yields after wildland fire in different rainfall regimes in the western United States. *International Journal of Wildland Fire* **18**(1): 96–115.

Moody JA, Shakesby RA, Robichaud PR, Cannon SH, Martin DA. 2013. Current research issues related to post-wildfire runoff and erosion processes. *Earth-Science Reviews* **122**: 10–37. https://doi.org/10.1016/j.earscirev.2013.03.004.

Nayak A, Marks D, Chandler DG, Seyfried M. 2010. Long-term snow, climate, and streamflow trends at the Reynolds Creek Experimental Watershed, Owyhee Mountains, Idaho, United States. *Water Resources Research* **46**(6): W06519, 1–15. https://doi.org/10.1029/2008WR007525.

Nearing MA, Simanton JR, Norton LD, Bulygin SJ, Stone J. 1999. Soil erosion by surface water flow on a stony, semiarid hillslope. *Earth Surface Processes and Landforms* **24**(8): 677–686.

Ott RL, Longnecker MT. 2010. *An Introduction to Statistical Methods and Data Analysis*, 6th edn. Nelson Education: Norwich, UK.

Pierce J, Meyer GA, Jull AJT. 2004. Fire-induced erosion and millennial scale climate change in northern ponderosa pine forests. *Nature* **432**: 87–90.

Pierson FB, Wight JR. 1991. Variability of near-surface soil temperature on sagebrush rangeland. *Journal of Range Management* **44**(5): 491–497.

Pierson FB, Williams CJ. 2016. *Ecohydrologic impacts of rangeland fire on runoff and erosion: a literature synthesis*, General Technical Report RMRS-GTR-351. US Department of Agriculture, Forest Service, Rocky Mountain Research Station: Fort Collins, CO.

Pierson FB, Blackburn WH, Vanvactor SS, Wood JC. 1994a. Partitioning small scale spatial variability of runoff and erosion on sagebrush rangeland. *Water Resources Bulletin* **30**(6): 1081–1090.

Pierson FB, Jr, Van Vactor SS, Blackburn WH, Wood JC. 1994b. Incorporating small scale spatial variability into predictions of hydrologic response on sagebrush rangelands. In *Variability in Rangeland Water Erosion Processes*, Blackburn WH, Pierson FB, Schuman GE, Zartman R (eds), Soil Science Society of America Special Publication 38. Soil Science Society of America: Madison, WI; 22–34.

Pierson FB, Slaughter CW, Cram ZK. 2000. *Monitoring discharge and suspended sediment, Reynolds Creek Experimental Watershed,*

Idaho, USA, ARS Technical Bulletin NWRC-2000-8. US Department of Agriculture, Agricultural Research Service, Northwest Watershed Research Center: Boise, ID.

Pierson FB, Slaughter CW, Cram ZK. 2001a. Long-term stream discharge and suspended-sediment database, Reynolds Creek Experimental Watershed, Idaho, United States. *Water Resources Research* **37**(11): 2857–2861.

Pierson FB, Robichaud PR, Spaeth KE. 2001b. Spatial and temporal effects of wildfire on the hydrology of a steep rangeland watershed. *Hydrological Processes* **15**(15): 2905–2916. https://doi.org/10.1002/hyp.381.

Pierson FB, Carlson DH, Spaeth KE. 2002. Impacts of wildfire on soil hydrological properties of steep sagebrush-steppe rangeland. *International Journal of Wildland Fire* **11**(2): 145–151.

Pierson FB, Robichaud PR, Moffet CA, Spaeth KE, Hardegree SP, Clark PE, Williams CJ. 2008a. Fire effects on rangeland hydrology and erosion in a steep sagebrush-dominated landscape. *Hydrological Processes* **22**(16): 2916–2929. https://doi.org/10.1002/hyp.6904.

Pierson FB, Robichaud PR, Moffet CA, Spaeth KE, Williams CJ, Hardegree SP, Clark PE. 2008b. Soil water repellency and infiltration in coarse-textured soils of burned and unburned sagebrush ecosystems. *Catena* **74**: 98–108.

Pierson FB, Moffet CA, Williams CJ, Hardegree SP, Clark PE. 2009. Prescribed-fire effects on rill and interrill runoff and erosion in a mountainous sagebrush landscape. *Earth Surface Processes and Landforms* **34**(2): 193–203. https://doi.org/10.1002/esp.1703.

Pierson FB, Williams CJ, Kormos PR, Hardegree SP, Clark PE, Rau BM. 2010. Hydrologic vulnerability of sagebrush steppe following pinyon and juniper encroachment. *Rangeland Ecology & Management* **63**(6): 614–629. https://doi.org/10.2111/rem-d-09-00148.1.

Pierson FB, Williams CJ, Hardegree SP, Weltz MA, Stone JJ, Clark PE. 2011. Fire, plant invasions, and erosion events on western rangelands. *Rangeland Ecology & Management* **64**(5): 439–449. https://doi.org/10.2111/rem-d-09-00147.1.

Robichaud PR. 2009. Post-fire stabilization and rehabilitation. In *Fire Effects on Soils and Restoration Strategies*, Cerdà A, Robichaud PR (eds), Vol. **5**, Land Reconstruction and Management Series. Science Publishers: Enfield, NH; 299–320.

Robichaud PR, Brown RE. 2002. *Silt fences: an economic technique for measuring hillslope soil erosion. General Technical Report RMRS-GTR-94*. US Department of Agriculture, Forest Service, Rocky Mountain Research Station: Fort Collins, CO.

Robichaud PR, Wagenbrenner JW, Lewis SA, Ashmun LE, Brown RE, Wohlgemuth PM. 2013a. Post-fire mulching for runoff and erosion mitigation. Part II. Effectiveness in reducing runoff and sediment yields from small catchments. *Catena* **105**: 93–111.

Robichaud PR, Lewis SA, Wagenbrenner JW, Ashmun LE, Brown RE. 2013b. Post-fire mulching for runoff and erosion mitigation. Part I. Effectiveness at reducing hillslope erosion rates. *Catena* **105**: 75–92.

Runkel RL, Crawford CG, Cohn TA. 2004. *Load Estimator (LOADEST): A FORTRAN Program for Estimating Constituent Loads in Streams and Rivers (Techniques and Methods 4-A5)*. US Department of Interior, Geological Survey: Reston, VA.

Salih MSA, Taha FK, Payne GF. 1973. Water repellency of soils under burned sagebrush. *Journal of Range Management* **26**: 330–331.

Sankey JB, Germino MJ, Glenn NF. 2009a. Aeolian sediment transport following wildfire in sagebrush steppe. *Journal of Arid Environments* **73**(10): 912–919.

Sankey JB, Germino MJ, Glenn NF. 2009b. Relationships of post-fire aeolian transport to soil and atmospheric conditions. *Aeolian Research* **1**(1–2): 75–85. https://doi.org/10.1016/j.aeolia.2009.07.002.

Sankey JB, Germino MJ, Benner SG, Glenn NF, Hoover AN. 2012a. Transport of biologically important nutrients by wind in an eroding cold desert. *Aeolian Research* **7**: 17–27.

Sankey JB, Germino MJ, Glenn NF. 2012b. Dust supply varies with sagebrush microsites and time since burning in experimental erosion events. *Journal of Geophysical Research, G: Biogeosciences* **117**(1): 1–13, G01013. https://doi.org/10.1029/2011jg001724.

SAS Institute Inc. 2013. *SAS version 9.4*. SAS Institute: Cary, NC.

Seyfried MS, Wilcox BP. 1995. Scale and the nature of spatial variability: field examples having implications for hydrologic modeling. *Water Resources Research* **31**(1): 173–184.

Seyfried MS, Harris RC, Marks D, Jacob B. 2000. *A geographic database for watershed research, Reynolds Creek Experimental Watershed, Idaho, USA*, ARS Technical Bulletin NWRC-2000-3. US Department of Agriculture, Agricultural Research Service, Northwest Watershed Research Center: Boise, ID.

Seyfried M, Harris R, Marks D, Jacob B. 2001. Geographic database, Reynolds Creek Experimental Watershed, Idaho, United States. *Water Resources Research* **37**(11): 2825–2829.

Seyfried MS, Grant LE, Marks D, Winstral A, McNamara J. 2009. Simulated soil water storage effects on streamflow generation in a mountainous snowmelt environment, Idaho, USA. *Hydrological Processes* **23**(6): 858–873.

Seyfried M, Lohse K, Marks D, Flerchinger G, Pierson F, Holbrook WS. 2018. Reynolds Creek Experimental Watershed and critical zone observatory. *Vadose Zone Journal* **17**(1): 1–20, 180129. https://doi.org/10.2136/vzj2018.07.0129.

Shakesby RA. 2011. Post-wildfire soil erosion in the Mediterranean: review and future research directions. *Earth-Science Reviews* **105**(3–4): 71–100. https://doi.org/10.1016/j.earscirev.2011.01.001.

Shakesby RA, Doerr SH. 2006. Wildfire as a hydrological and geomorphological agent. *Earth-Science Reviews* **74**(3–4): 269–307.

Slaughter CW, Marks D, Flerchinger GN, Van Vactor SS, Burgess M. 2001. Thirty-five years of research data collection at the Reynolds Creek Experimental Watershed, Idaho, United States. *Water Resources Research* **37**(11): 2819–2823.

Snyder KA, Evers L, Chambers JC, Dunham J, Bradford JB, Loik ME. 2019. Effects of changing climate on the hydrological cycle in cold desert ecosystems of the Great Basin and Columbia Plateau. *Rangeland Ecology & Management* **72**(1): 1–12.

Spigel KM, Robichaud PR. 2007. First-year post-fire erosion rates in Bitterroot National Forest, Montana. *Hydrological Processes* **21**(8): 998–1005.

Stephenson GR. 1977. *Soil–geology–vegetation inventories for Reynolds Creek Watershed*, Miscellaneous series No. 42. University of Idaho, College of Agriculture, Agricultural Experiment Station: Moscow, ID.

USDA-ARS-NWRC. 2015. Public database for the Reynolds Creek Experimental Watershed. US Department of Agriculture, Agricultural Research Service, Northwest Watershed Research Center: Boise, ID. Available: ftp://ftp.nwrc.ars.usda.gov/publicdatabase/reynolds-creek/ access date 20 February 2018.

USDA-ARS-NWRC. 2016. Public database for the Reynolds Creek Experimental Watershed. US Department of Agriculture, Agricultural Research Service, Northwest Watershed Research Center: Boise, ID. Available: ftp://ftp.nwrc.ars.usda.gov/publicdatabase/reynolds-creek/ access date 20 February 2018.

USDA-ARS-NWRC. 2017. Public database for the Reynolds Creek Experimental Watershed. US Department of Agriculture, Agricultural Research Service, Northwest Watershed Research Center: Boise, ID. Available: ftp://ftp.nwrc.ars.usda.gov/publicdatabase/reynolds-creek/

USDI-BLM. 2016. *Soda Fire: emergency stabilization and rehabilitation, Idaho and Oregon*. US Department of Interior, Bureau of Land Management: Owhyee County, ID.

Vega SP. 2018. Post-fire soil erosion patterns and processes in a complex sagebrush rangeland watershed. Master's thesis. University of Idaho, Moscow, ID.

Wagenbrenner NS, Germino MJ, Lamb BK, Robichaud PR, Foltz RB. 2013. Wind erosion from a sagebrush steppe burned by wildfire: measurements of PM_{10} and total horizontal sediment flux. *Aeolian Research* **10**: 25–36. https://doi.org/10.1016/j.aeolia.2012.10.003.

Wilcox BP, Breshears DD, Allen CD. 2003. Ecohydrology of a resource-conserving semiarid woodland: effects of scale and disturbance. *Ecological Monographs* **73**(2): 223–239.

Wilcox BP, Turnbull L, Young MH, Williams CJ, Ravi S, Seyfried MS, Bowling DR, Scott RL, Germino MJ, Caldwell TG, Wainwright J. 2012. Invasion of shrublands by exotic grasses: ecohydrological consequences in cold versus warm deserts. *Ecohydrology* **5**(2): 160–173. https://doi.org/10.1002/eco.247.

Williams CJ, McNamara JP, Chandler DG. 2009. Controls on the temporal and spatial variability of soil moisture in a mountainous landscape: the signature of snow and complex terrain. *Hydrology and Earth System Sciences* **13**(7): 1325–1336.

Williams CJ, Pierson FB, Robichaud PR, Boll J. 2014a. Hydrologic and erosion responses to wildfire along the rangeland-xeric forest continuum in the western US: a review and model of hydrologic vulnerability. *International Journal of Wildland Fire* **23**(2): 155–172. https://doi.org/10.1071/wf12161.

Williams CJ, Pierson FB, Al-Hamdan OZ, Kormos PR, Hardegree SP, Clark PE. 2014b. Can wildfire serve as an ecohydrologic threshold-reversal mechanism on juniper-encroached shrublands? *Ecohydrology* **7**(2): 453–477. https://doi.org/10.1002/eco.1364.

Williams CJ, Pierson FB, Robichaud PR, Al-Hamdan OZ, Boll J, Strand EK. 2016a. Structural and functional connectivity as a driver of hillslope erosion following disturbance. *International Journal of Wildland Fire* **25**(3): 306–321.

Williams CJ, Pierson FB, Kormos PR, Al-Hamdan OZ, Hardegree SP, Clark PE. 2016b. Ecohydrologic response and recovery of a semiarid shrubland over a five year period following burning. *Catena* **144**: 163–176. https://doi.org/10.1016/j.catena.2016.05.006.

Winstral A, Marks D, Gurney R. 2013. Simulating wind-affected snow accumulations at catchment to basin scales. *Advances in Water Resources* **55**: 64–79. https://doi.org/10.1016/j.advwatres.2012.08.011.

Ziegenhagen LL, Miller RF. 2009. Postfire recovery of two shrubs in the interiors of large burns in the Intermountain West USA. *Western North American Naturalist* **69**(2): 195–205.